Inhalable antibiotic prodrug therapies for the treatment of intracellular pulmonary infections

Abby M Kelly

A thesis

submitted in partial fulfillment of the

requirements for the degree of

Master of Science

University of Washington

2017

Reading Committee:

Patrick Stayton, Chair

Daniel Ratner

Program Authorized to Offer Degree:

Bioengineering

University of Washington

Abstract

Inhalable antibiotic prodrug therapies for the treatment of intracellular pulmonary infections

Abby M Kelly

Chair of the Supervisory Committee:
Professor Patrick S. Stayton
Bioengineering

One hundred years after the discovery of antimicrobials and antibiotics, lower respiratory infections remain one of the leading causes of death worldwide. Infectious agents such as *Francisella tularensis* and *Burkholderia pseudomallei* contribute to this burden as the causative agents of pulmonary tularemia and melioidosis, respectively. These pathogens cause substantial morbidity and mortality and due to their aerosolizability are weaponizable pathogens for bio-warfare. As such, the Centers for Disease Control and Prevention classify them as Tier 1 threat agents. Current care of these intracellular lung infections relies solely on weeks to months of intravenous and/or oral antibiotic delivery. Yet, 10-20% of patients die following treatment and another 5-10% relapse. These clinical failures are due to poor drug biodistribution within the lungs and low bioavailability, with potential off-target side effects due to systemic delivery. Inhalable delivery platforms aim to overcome these problems through direct delivery of antibiotics to the sight of infection. Systems such as inhalable free drug dispersions and

antibiotics encapsulated within liposomal formulations are under investigation, however these systems fail to control drug pharmacokinetics often delivery a burst release, and often require complex formulations hampering large scale production and regulatory approval.

Previous work in the Stayton lab, including work presented in this thesis, helped lay the foundation of a macromolecular inhalable prodrug platform utilizing RAFT polymerization of a ciprofloxacin (cipro) prodrug monomer towards the treatment of pulmonary tularemia. Initial co-monomer investigations were performed with polyethylene glycol methacrylate (PEGMA), carboxybetaine methacrylate, and mannose methacrylate monomers. These co-monomers were investigated for their ability to aid in drug solubility, loading, stability, biocompatibility, and in the case of the mannose monomer, for it's targeting capabilities to surface receptors on alveolar macrophage. This foundational work lead to PEGMA-cipro polymers capable of prolonging survival in a lethal murine *F. novicida* infection model in 70% of mice to the experimental endpoint at 14 days post infection over untreated mice with 0% survival at just 4 days post infection following a 3 day treatment dosing schedule. The carboxybetaine co-monomer was only ever investigated in vitro, but was shown to be nontoxic, produce excellent drug solubility and loading, and increase cellular internalization over similar PEGMA polymers. However, the mannose co-monomer unexpectedly outperformed both the PEGMA and carboxybetaine co-monomers. The Mannose-Cipro polymers were shown to increase animal survival to 90% at 16 days post infection, compared to 0% survival in untreated mice at 8-10 days post infection following a 3 day treatment dosing schedule. Additionally, the mannose monomer was shown to increase cellular uptake by alveolar macrophage via receptor-mediated endocytosis, and provide excellent drug solubility, loading, and biocompatibility.

Following this strong foundation, a second antibiotic prodrug monomer was synthesized from meropenem. Meropenem is the drug of choice in the treatment of melioidosis and is currently not available in any format other than injectable. This novel meropenem monomer was synthesized utilizing the same hydrolysable linker as the ciprofloxacin monomer for it's optimal pharmacokinetic profile. The meropenem monomer was copolymerized via RAFT with the mannose-methacrylate co-monomer, and much of its in vitro characterization has been completed. This novel polymer is completely nontoxic in culture to the highest concentration evaluated (10 mg/mL), a dose at which the mannose-cipro polymer causes 50% cell death, indicating excellent biocompatibility. The polymer is also highly bactericidal in an intracellular coculture infection assay against the model bacterium *B. thailandensis*, with similar activity as the mannose-cipro polymer. Additionally, a terpolymer has been synthesized comprised of mannose, meropenem, and ciprofloxacin that is equally nontoxic but with enhanced bactericidal activity in culture. While drug combination analysis between meropenem and ciprofloxacin is so far inconclusive, the terpolymer activity suggests meropenem and ciprofloxacin have synergistic mechanisms of action against *B. thailandensis* and may be highly effective at combating pulmonary melioidosis in the form of combination therapies.

TABLE OF CONTENTS

List of Figures iii

List of Tables iv

Chapter 1. Introduction 8

1.1 Intracellular Pulmonary Infections: Tularemia & Melioidosis 9

1.2 Current Standard of Care 11

1.3 Pulmonary Delivery Strategies to Improve Treatment Outcomes 13

1.3.1 Free antibiotic delivery 13

1.3.2 Drug encapsulation: Liposomes & Polymersomes 14

1.3.3 An Inhalable Macromolecular Prodrug Platform: A Brief History 16

1.4 Project Goals 20

Chapter 2. Inhalable mannose-meropenem drugamers point towards combination therapies against pulmonary melioidosis 21

2.1 Abstract 21

2.2 Introduction 22

2.3 Materials & Methods 24

2.3.1 Materials 24

2.3.2 Synthesis of meropenem carbamate methacrylate (MCM) prodrug monomer 25

2.3.3 Synthesis of ciprofloxacin tyramine methacrylate (CTM) prodrug monomer 27

2.3.4 Synthesis of mannose ethyl methacrylate (MEM) targeting monomer 28

2.3.5 RAFT polymerization of poly($MEM_{co}MCM$), poly($MEM_{co}CTM$), and poly($MEM_{co}MCM_{co}CTM$) 30

2.3.6 Drug Release Kinetic Analysis via HPLC 31
2.3.7 In vitro Cytotoxicity Analysis 32
2.3.8 In vitro Co-culture, Intracellular Infection Efficacy Analysis 33
2.3.9 Drug Combination Analysis against *Burkholderia thailandensis* 33
2.4 Results & Discussion 35
2.4.1 RAFT polymerization and polymer characterization 35
2.4.2 Drug Release Kinetics via HPLC: Challenges & Future Studies 37
2.4.3 In vitro cytotoxicity Analysis via MTS Assay 40
2.4.4 In vitro Bactericidal Efficacy via Coculture Mammalian Cell Infection Assay 41
2.4.5 Antibiotic Combination Analysis in a *B. thailandensis* Planktonic Assay 43
2.5 Conclusions 45
2.6 Acknowledgements 46
Chapter 3. Future Work 47
3.1 In vivo analysis 47
3.2 Combination therapies 50
Bibliography 51

LIST OF FIGURES

Figure 1.1. World Health Organization Top 10 Causes of Death ……...…8

Figure 1.2. Deposition of delivered dye via installation vs. aerosolization ……....…13

Figure 1.3. Formulation of drug encapsulating liposomes (or polymersomes)… ……14

Scheme 1.1. Synthesis scheme for carboxybetaine-ciprofloxacin polymers ……18

Figure 1.4. Summary of Carboxybetaine data. ……19

Scheme 2.1. Synthesis Scheme for the meropenem carbamate methacrylate (MCM) prodrug monomer……...…25

Scheme 2.2: Strategy for synthesis of poly(MEMcoMCM) via RAFT polymerization……...……35

Figure 2.1: Polymer Characterization via ^{1}H-NMR ……..……36

Figure 2.2: HPLC Meropenem Standard Curves ……..……38

Figure 2.3: in vitro cytotoxicity analysis via MTS assay ……..……..…40

Figure 2.4: in vitro mammalian cell intracellular infection coculture assay ……..……41

Figure 2.5: Bactericidal activity of free meropenem vs. ciprofloxacin ……..……...…42

Figure 2.6: Isobologram analysis of checkerboard drug combination assay data.……44

Figure 3.1: In vivo gross toxicity analysis of poly(MEM$_{co}$MCM)……48

LIST OF TABLES

Table 2.1. RAFT polymerization reagent values ……31

ACKNOWLEDGEMENTS

I would like to acknowledge the hard work of several people who contributed greatly to the work presented in this thesis and who have supported me during my time at the University of Washington. First and foremost, Dr. Anthony Convertine and Dr. Selvi Srinivasan, thank you for your tireless work and chemistry brilliance, for designing, troubleshooting, and synthesizing the polymers and monomers presented here. Thank you to my fellow Stayton labmates and collaborators past and present for your friendship, support, and knowledge; Dr. Hanna Kern, Dr. David Chui, Dr. Hye-Nam Son, Dr. Jasmin Chen, Dr. Debobrato 'Jojo' Das, Fang-Yi 'Ida' Su, Christine Yoo, Brian Lee, Dr. Kate Montgomery, Dr. Clare LeGuyader, and James Rushworth. You've all made life so much more enjoyable and productive these past three years. Finally, I'd like to thank the two most important people of my UW experience, Dr. Patrick Stayton and Dr. Daniel Ratner. Thank you both for your brilliance and hard work, for putting together the funding and research team that made this work possible, and for your guidance and support throughout.

In addition to the wonderful people at UW, I'd also like to acknowledge a number of people at the Commonwealth Science and Industry Research Organization. I'd like to thank Dr. John Chiefari, Dr. Kathy Turner, Dr. Kristine Barlow, and Dr. Almar Postma for welcoming me, making me feel at home in Australia, and for helping me greatly with my research when everything seemed to go wrong. I'd especially like to thank Dr. Katherine Lockock, Dr. Wioleta Kowalczyk, and Dr. Greg Simpson, not just for welcoming me to Australia and helping me with my research, but for your kindness, friendship, and continuing support; I miss you all so much!

Last but not least, I need to acknowledge two outstanding organizations without which none of the amazing experiences of the last 5 years of my life would have occurred; the National

Science Foundation for supporting my research with a Graduate Research Fellowship, and the Fulbright program for supporting a year of research at CSIRO in Melbourne, Australia with a postgraduate research scholarship. I feel so fortunate and owe so much to these programs!

DEDICATION

This work is dedicated to my husband, Ben and our son, Harrison who support me always and love me unconditionally. These past few years would have been impossible without you and the wonderful things that lay ahead will be all the sweeter because of you!!! It's finally time to put family first.

Chapter 1. INTRODUCTION

The first antimicrobial compound was developed in 1911 and by the late 1920s and early 1930s antibiotics were in widespread use, leading to cures for numerous infectious diseases previously considered incurable [3]. Yet, a century later, infectious diseases are still among the top causes of death worldwide. According to the World Health Organization, lower respiratory infections top the list for causes of death in low-income economies and rank 3rd worldwide [**Figure 1.1**] [1]. The challenges of treating lower respiratory infections are as varied as the microbial agents that cause them. Most of the attention in recent years has been on the emergence of antibiotic resistance. In 2014, President Barack Obama gave an executive order to

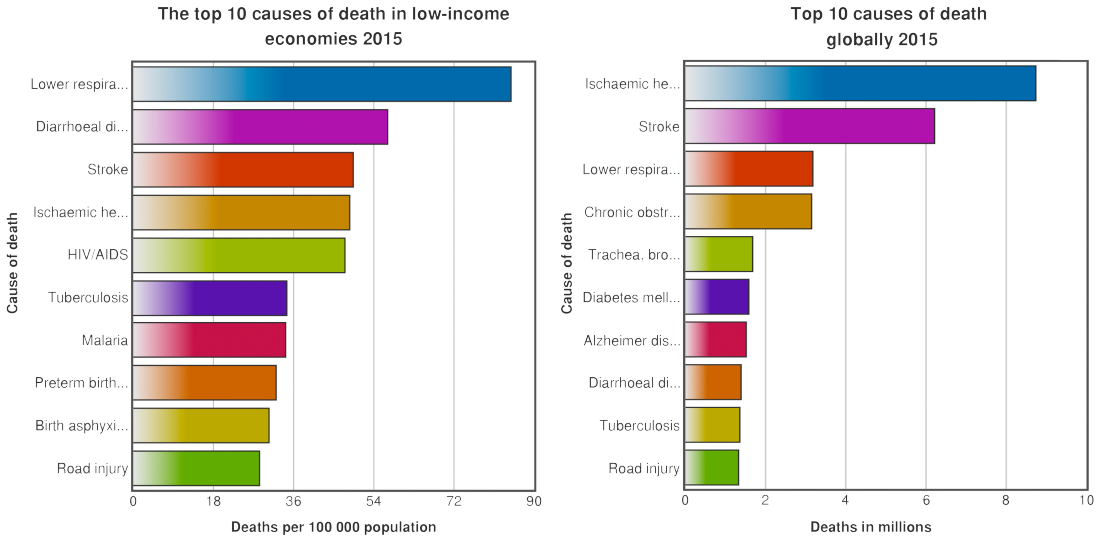

Figure 1.1. World Health Organization Top 10 Causes of Death [1] (a) in low-income economies of the world and (b) globally. Compiled from 2015 data, these data show the prevalence of lower respiratory infections and their impact on human mortality worldwide.

address the challenges of antibiotic resistance at a national level, including additional development of a task force and a call for increased research funding [4]. The first actionable point of this order was to develop methods to slow the development of antibiotic-resistance, and from that action and outreach by the Centers for Disease Control (CDC) many efforts have been made

by researchers and clinicians to limit antibiotic use and dosages wherever possible [5]. In addition to the emergence of antibiotic-resistance in bacteria, additional challenges in the treatment of lower respiratory infections involve unique challenges in combating specific microbial pathogens. Most challenging are intracellular pathogens with immunomodulatory mechanisms such as the causative agents of pulmonary tularemia and melioidosis.

1.1 Intracellular Pulmonary Infections: Tularemia & Melioidosis

Tularemia and melioidosis are bacterial infections caused by *Francisella tularensis* and *Burkholderia pseudomallei*, respectively. These infections can be acquired via multiple routes such as through cuts or scrapes on the skin or ingestion, but inhalation causes the highest rates of morbidity and mortality. *F. tularensis* is a zoonotic bacteria carried by insects and animals, as such the majority of naturally occurring tularemia cases are of the ulceroglandular form caused by insect bites [6]. Pulmonary tularemia, or pneumonic tularemia, is more rare, but far more deadly. The inhaled form of tularemia presents as pneumonia with fever, body aches, bronchitis, and lung ulcers, swelling, and hemorrhage [7, 8]. As few as 10 colony forming units (CFU), or individual bacteria cells, are sufficient to cause pulmonary tularemia leading to a 30-40% mortality rate when untreated [7, 9].

Unlike *F. tularensis*, *B. pseudomallei* is a saprophyte, deriving it's nutrients from decaying matter and is found prevalently in soil and waterways [10, 11]. As such, melioidosis is most frequent in tropical regions where soil and water become aerosolized during the rainy season and bacteria are readily inhaled, making the pulmonary variety of melioidosis endemic in these regions. Pulmonary melioidosis, like pneumonic tularemia, also causes pneumonia-like symptoms including lung abscesses, empyema, and can lead to chronic lung disease and sepsis. The ability of *B. pseudomallei* to disseminate throughout the body makes pulmonary melioidosis

far more dangerous than pulmonary tularemia, as well as difficult to treat. Without treatment, mortality rates for pulmonary melioidosis are between 40-80%, depending on the presence of sepsis, and even with treatment mortality is between 10-20% and relapse occurs in 5-10% of cases [10, 12-15].

Both *F. tularensis* and *B. pseudomallei* are gram negative, intracellular pathogens, infecting multiple cell types within the lungs upon inhalation, particularly alveolar macrophage [6, 7, 10, 15]. Both bacteria evade the host immune response by replicating within the very cells typically responsible for clearing the body of foreign pathogens, although the precise mechanisms differ. *F. tularensis* can internalize into macrophage by phagocytosis or by activation of the mannose receptors. Phagocytosis is the mechanism by which macrophage clear bacterial or fungal pathogens from the body, however *F. tularensis* is capable of preventing the normal acidification of the phagosome [16-18], thus survive degradation. The mechanisms of phagosomal and endosomal escape have yet to be fully elucidated [18]. Alternatively, *F. tularensis* are also capable of evading opsonization and macrophage phagocytosis altogether by activation of mannose receptors on the macrophage cell surface and subsequent receptor-mediated internalization [16, 17]. An additional feature of *F. tularensis* immune evasion lies in its atypical lipopolysaccharide (LPS), which prevents typical recognition by host toll-like receptors [19, 20]. Once internalized, *F. tularensis* replicates within the cytosol very rapidly, increasing in number by 1.5-2.5 log in just 24 hours [21].

B. pseudomallei is also capable of preventing opsonization and subsequent degradation within the macrophage phagosomal pathway, but by synthesizing an extracellular polysaccharide capsule that limits the bacterial interaction with the host compliment system [22, 23]. Upon endocytosis, B. pseudomallei are capable of lysing the endosomal membrane to enter the cytosol

[24]. While *F. tularensis* must lyse its host cell in order to infect adjacent cells, *B. pseudomallei* have adapted a unique infection mechanism that allows the pathogen to continue evasion of the host immune system. These clever bacteria can polymerize actin, which fuses with the host membrane and protrudes an actin filament between macrophage providing *B. pseudomallei* a channel to infect a neighboring cell without lysing it's initial host cell or ever reentering the extracellular space [25, 26].

The extreme pathogenicity, morbidity, and mortality associated with pulmonary tularemia and melioidosis combined with the ability of both pathogens to be aerosolized make *F. tularensis* and *B. pseudomallei* attractive agents of bio-terrorism and bio-warfare [8, 27, 28]. Due to the high casualties predicted upon release of these pathogens in the event of a bioterrorist attack, the DHHS, CDC, and USDA consider both pathogens tier 1 threat agents [29, 30]. This threat is particularly high for US soldiers deployed in the field, who are prime targets of bioterrorism but have limited access to rapid treatment. Preparedness strategies must include the ability to deploy treatment rapidly, strategies for pre and post-exposure prophylaxis, therapeutics that are easily scaled for mass production, and a high degree of drug stability for both stock-piling and deployment in the field [31, 32]. Current care for both tularemia and melioidosis are severely lacking, in their ability to effectively treat the natural occurrences of infection as well as in the event of a bioterrorist attack.

1.2 Current Standard of Care

The current standard of care for tularemia and melioidosis involve weeks to months of intravenous and/or oral antibiotic delivery. For pulmonary tularemia, oral antibiotics taken for 1-4 weeks are standard, with IV administration reserved for the most advanced cases. Antibiotics of choice include aminoglycosides (streptomycin and gentamicin), and fluoroquinolones

(ciprofloxacin) [7, 33, 34]. For pulmonary melioidosis, due to the potential for bacterial dissemination throughout the body and it's high mortality, IV antibiotic administration is the first line of defense lasting from 2-6 weeks followed by oral antibiotic administration for up to three months. The antibiotics of choice are the carbapenems (meropenem and imipenem) for IV delivery followed by the cephalosporin, ceftazidime for oral administration [11, 12].

One of the primary challenges in the treatment of pulmonary tularemia lies in the difficulty of diagnosis. Because the disease presents as pneumonia, it's often mistake for a *Streptococcus pneumonia* infection, which is the most common bacterial pneumonia [35]. This combined with the rapid replication of *F. tularensis* and its high pathogenicity (requiring just 10 CFUs to cause infection) cause much of its associated mortality. Pulmonary melioidosis is similarly difficult to diagnose. The disease can mimic other infections like typhoid fever, tuberculosis, or glanders [10, 13, 36]. Additional challenges lie in the ability of *B. pseudomallei* to disseminate from the lungs causing sepsis and its resistance to most antibiotics, including penicillin, ampicillin, and most cephalosporins and aminoglycosides [12, 37].

Better culture techniques to more rapidly and safely, diagnose pulmonary tularemia and melioidosis are under investigation [38, 39], but improving treatment outcomes and preparing for a potential bioterrorist threat also require dramatic improvements in the delivery of the antibiotics themselves.

1.3 PULMONARY DELIVERY STRATEGIES TO IMPROVE TREATMENT OUTCOMES

1.3.1 **Free antibiotic delivery**

There are multiple problems with systemic delivery of free antibiotics, such as poor biodistribution within the lungs, poor drug bioavailability, and rapid clearance necessitating high dosages that often cause off-target side effects [40-42]. One approach to improve drug biodistribution and reduce the necessary drug dose is to deliver antibiotics directly to the lungs. This can be facilitated by techniques such as intranasal instillation, intratracheal injection, or aerosolization with the later providing deeper, more distributed delivery [**Figure 1.2**] (unpublished figure) and ease of administration via nebulizer or inhaler. A few FDA approved

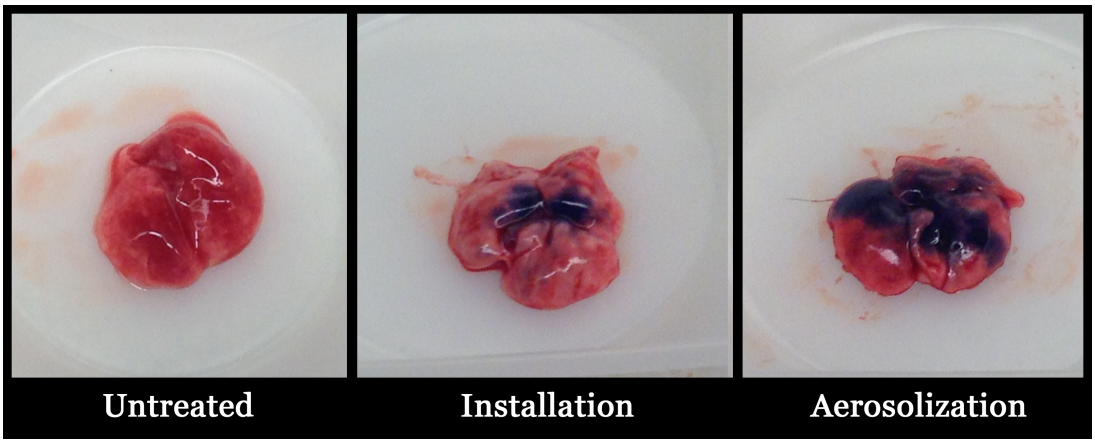

Figure 1.2: Deposition of delivered dye via installation vs. aerosolization: A solution of 0.2% [w/v] of Brilliant blue R250 in 1x PBS was delivered to black 6 mice via intratracheal installation and microsprayer aerosolization and mice were immediately sacked and lungs harvested for comparison.

formulations are currently on the market for the treatment of cystic fibrosis related infections. Novartis has a formulation of tobramycin (TOBI®) and Gilead has a formulation of azteonam monobactum (Cayston®), both delivered by nebulizer. These formulations report a 10% improvement in lung function over placebo controls, their efficacy hindered by poor pharmacokinetics in the lungs [43-47]. Adequate aerosol deposition in diseased lungs is often obstructed by excess mucus in the bronchi and bronchioles, and the issues of rapid drug

clearance and poor drug bioavailability associated with systemic delivery remain unaddressed [48]. An additional limitation of free drug delivery is the poor solubility of hydrophilic drugs like ciprofloxacin, which is the current drug of choice in the treatment of tularemia [49, 50].

1.3.2 Drug encapsulation: Liposomes & Polymersomes

To address more of these limitations, various drug encapsulations strategies have been employed or are under investigation, most notably liposomes and polymersomes. These constructs are formulated from amphiphilic lipids or block copolymers that spontaneously form spherical bilayers or micelles under aqueous conditions due to the hydrophobic effect [51]. Both hydrophilic and hydrophobic drugs can easily be loaded into these structures, either within the aqueous core or entrapped in the hydrophobic bilayer [**Figure 1.3**, modified from [2]]. Liposomes have been used with varying degrees of success for the aerosolized delivery of ciprofloxacin. Aradigm is currently evaluating two liposomal formulations of ciprofloxacin against various

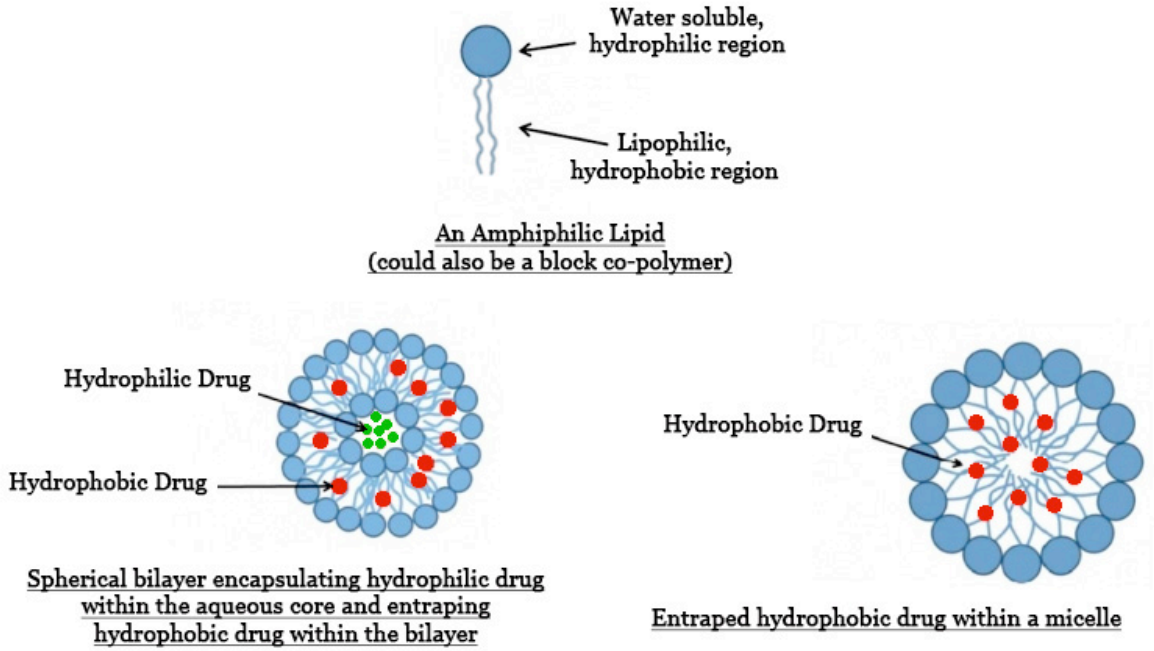

Figure 1.3: Formulation of drug encapsulating liposomes (or polymersomes) from amphiphilic molecules in aqueous solution [2]

types of pulmonary infection including *F. tularensis*. Their Lipoquin formulation, that have been shown to extend the half-life of ciprofloxacin from 2 hrs. following pulmonary delivery of free drug to 24 hours within the liposomal formulation. Additionally, the Lipoquin was able to improve animal survival in a lethal *F. tularensis* LV-Schu4 model over both oral ciprofloxacin delivery and aerosolized free ciprofloxacin delivery [52, 53]. While Lipoquin successfully increases drug bioavailability within the lungs, reduces the required ciprofloxacin dose, and increases animal survival the system remains flawed. Lipoquin fails to control drug release kinetics and has a classic burst release common to liposomal delivery [53]. Additionally, liposomal systems are often difficult to precisely reproduce thanks to complex formulations, making large-scale manufacturing and regulatory approval challenging [54-56].

Polymersome encapsulation provides better control over drug release kinetics compared to liposomal systems, as well as the ability to more easily modify the surface chemistry to add in additional functionality [57, 58]. The most widely used polymer in drug delivery is poly(lactic-co-glycolic) acid (PLGA) due to it's inherent biocompatibility, degradability under physiological conditions, and chemically modifiable carboxyl groups [59]. PLGA has been formulated with ciprofloxacin as an inhalable dry power for aerosolized lung delivery. These polymersomes contained <1 wt.% ciprofloxacin, but exhibited extended drug release with sustained release for 20 days in vitro [60]. While polymersomes offer control of drug loading/release over liposomes, they still suffer from formulation complexity and poor reproducibility, complicating large-scale manufacturing and regulatory approval [57, 61].

While encapsulation strategies address many of the issues with systemic drug delivery or pulmonary delivery of free antibiotics, formulation complexity and poor reproducibility, along with poor drug loading hamper the ability of these systems to adequately address all of the issues

with the treatment of pulmonary tularemia and melioidosis. Drug release can be further optimized by covalently linking the drug to the polymer via labile linkages to precisely release under desired stimuli. Covalent drug linkage also offers the added benefit of more precisely controlled drug loading and reduces batch variability and formulation complexity [41, 62]. The most common approach to link drugs to a polymer is a by post-polymerization conjugation strategies. While these strategies work well, they add additional and unnecessary steps to the synthesis process, which ultimately adds cost to the final therapeutic. An alternative, and more recent approach is the synthesis of prodrug monomers; chemically inactive drugs, modified with a labile linkage that connects the drug to a polymerizable functional group. Prodrug monomers can be polymerized directly into the system, require no additional post-conjugation steps, and become active upon cleavage of the labile linkage under the desired stimuli. This approach also improves drug loading and drug stability prior to release [63-65].

1.3.3 **An Inhalable Macromolecular Prodrug Platform: A Brief History**

In order to address all of the challenges towards combating intracellular pulmonary infections, a purely synthetic platform was developed. Ciprofloxacin prodrugs were synthesized using a similar approach to the synthesis of norfloxacin prodrugs already characterized in the literature [66, 67]. Reversible addition-fragmentation chain transfer (RAFT) polymerization was used as the synthesis method for it's ease, functionality with a wide range of monomers and different reaction conditions, and high degree of control over polymer size and dispersities [68, 69]. RAFT had also already been utilized to synthesize antibiotic prodrug delivery systems incorporating Ribavirin and poly(N-(2-hydroxypropyl) methacrylate) for the treatment of HIV and hepatitis C co-infections [70]. However, multiple factors required investigation including: 1) the optimal drug linkage to provide sustained drug release over a clinically relevant time period,

2) the optimal polymer architecture to provide biocompatibility, high drug loading, induce cellular internalization, and increase retention within the lungs, and 3) the optimal co-monomer(s) to confer high drug loading, stability, solubility, and biocompatibility.

Towards this end, Dr. Das was able to determine that a phenolic ester linkage hydrolyzed more rapidly than an aliphatic ester drug linkage [71] while providing near first order release kinetics sufficient to prolong mice survival in a lethal *F. novicida* infection model [72]. Those polymer systems utilized a poly(ethylene glycol) methacrylate (PEGMA) co-monomer to solubilize the hydrophobic ciprofloxacin prodrug monomer, and while the PEGMA performed well in vivo, Dr. Chen showed improved function with an alternative co-monomer.

While investigating the effects of glycan monomers as targeting moieties for alveolar macrophage attachment and internalization to improve intracellular delivery of the copolymerized ciprofloxacin, Dr. Chen observed the ability of the mannose monomer to efficiently solubilize ciprofloxacin and enhance drug loading every bit as efficiently as PEGMA, but while also inducing receptor mediated endocytosis and improved mice survival in the same lethal F. novicida model [73].

Concurrently with the PEGMA and mannose co-monomer research, investigation was also underway on the use of carboxybetaine as a zwiteronic co-monomer for ciprofloxacin delivery in the treatment of pulmonary tularemia [**Scheme 1.1**]. It was hypothesized that the positive and negative charge of carboxybetaine would reduce the slight toxicity of the ciprofloxacin that we suspected was due to its protonated secondary amine at physiological pH. Additionally, carboxybetaine has been shown to improve polymer retention time and does not seem to cause antibody production the way PEGMA does, implying it is less immunogenic [74, 75].

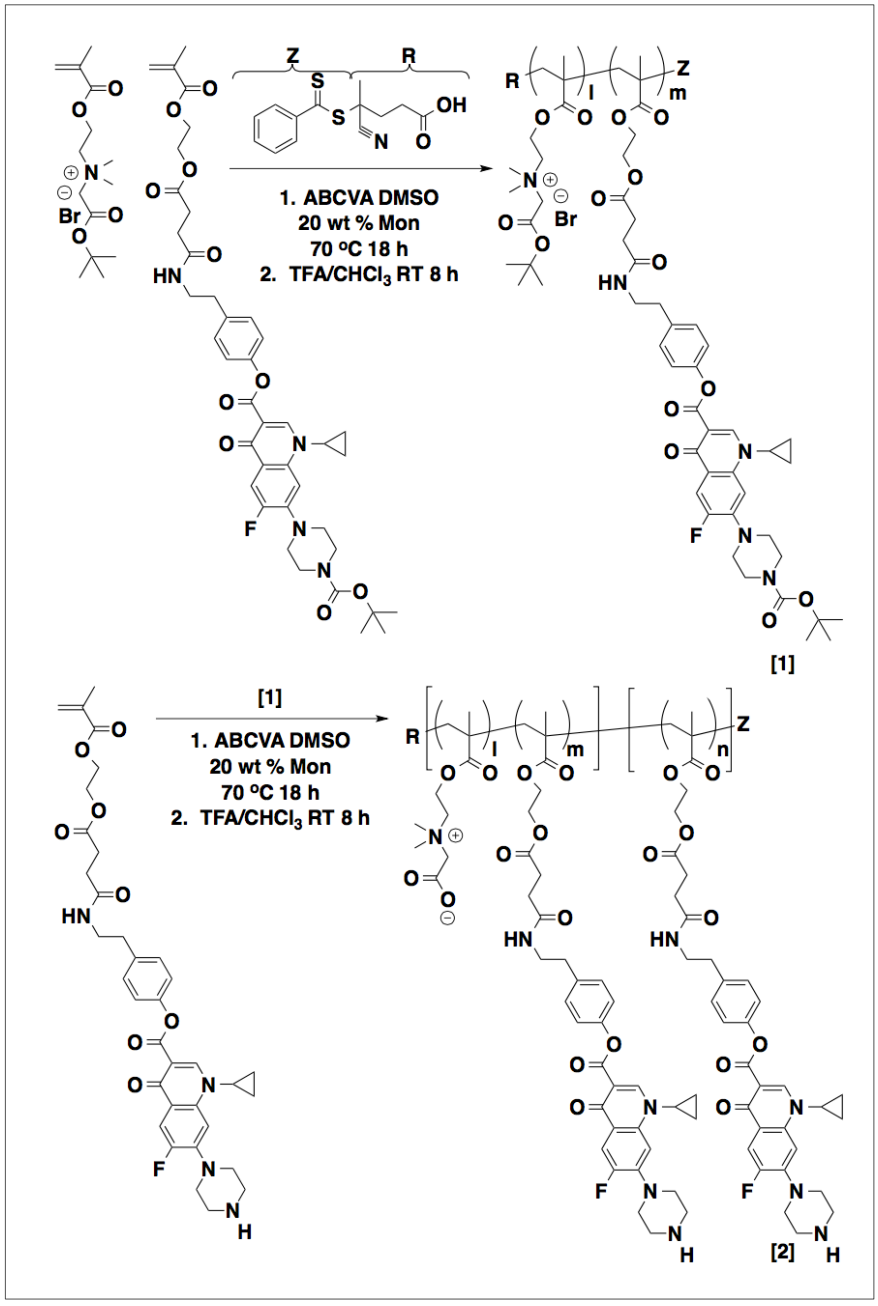

Scheme 1.1: Synthesis scheme for carboxybetaine-ciprofloxacin polymers. (top) synthesis of the linear copolymer, poly(CBM-co-CTM), and (bottom) synthesis of the block copolymer, poly(CBM-co-CTM)-b-CTM

Results for the carboxybetaine-ciprofloxacin polymers were promising. The systems showed tailored release kinetics based on polymer architecture, exhibited excellent biocompatibility in vitro and in vivo, good efficacy in vitro in a mammalian cell infection coculture model, and the

block copolymer showed increased cellular uptake by murine macrophage cells over the linear polymers [**Figure 1.4**, unpublished work]. However, due to the exceptional activity of the

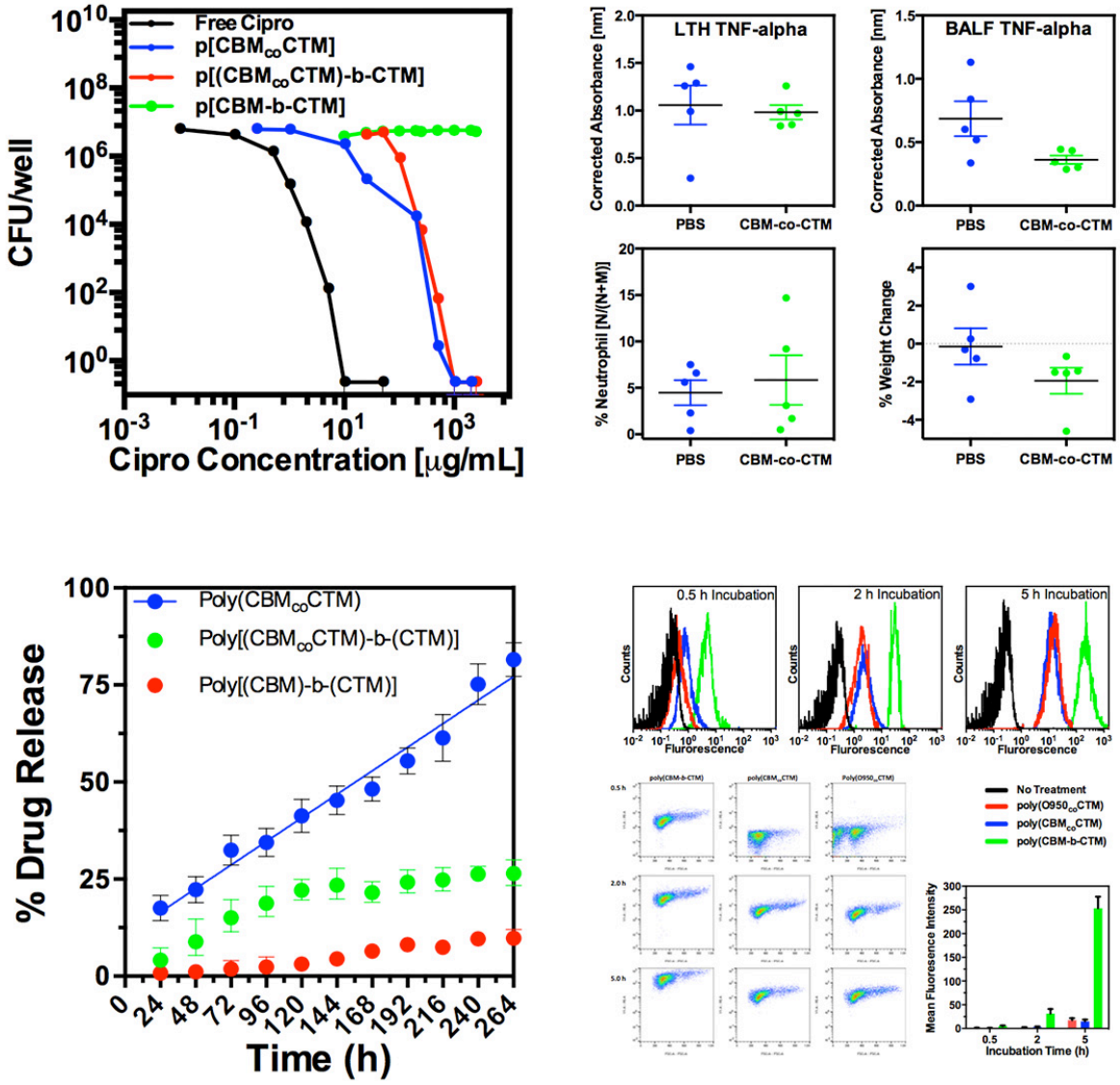

Figure 1.4: Summary of Carboxybetaine data. (top left) in vitro efficacy data collected using a mammalian infection coculture assay with *B. thailandensis*. The linear and block copolymers show good efficacy against intracellular infection, whereas the block polymer has no bactericidal activity. Free drug will always outperform polymeric cipro, as it freely diffuses across the cell membrane, (bottom left) drug release kinetic data from HPLC analysis shows the block polymer is releasing cipro too slowly to be efficacious in vitro, whereas the block copolymer shows faster release and the linear copolymer shows the fastest release with 80% of the total polymerized ciprofloxacin release in 264 hrs, (top right) in vivo toxicity markers following 3 repeated doses over 3 consecutive days of aerosolized delivery of 20 mg/kg polymerized ciprofloxacin within the linear copolymer in 50 μL of PBS, delivered to black 6 mice compared to PBS only control shows no statistical differences between polymer and control across all four markers of inflammation/toxicity, and (bottom right) cellular internalization of fluorescently labeled polymers after incubation with murine macrophage collected via flow cytometry shows the block copolymer is readily internalized by cells whereas the two linear polymers are not.

mannose co-monomer to induce receptor mediated endocytosis while maintaining excellent drug loading, stability, and biocompatibility, additional research was shifted to mannose copolymers.

1.4 PROJECT GOALS

The Ciprofloxacin prodrug monomer was originally created in part due to its ease of synthesis and the documented synthesis method for fluoroquinolone prodrug monomers, as well as its clinical use in the treatment of Tularemia. In order to apply the inhalable macromolecular prodrug platform to other diseases, specifically pulmonary melioidosis, new prodrug monomers must be synthesized, polymerized, and evaluated.

Towards this end, the goals of the work presented in this thesis are to evaluate the in vitro biocompatibility and bactericidal activity of novel mannose-meropenem prodrug polymers in an effort to optimize their in vivo performance potential.

Chapter 2. INHALABLE MANNOSE-MEROPENEM DRUGAMERS POINT TOWARDS COMBINATION THERAPIES AGAINST PULMONARY MELIOIDOSIS

2.1 ABSTRACT

Pulmonary melioidosis is an intracellular infection of the alveolar macrophage with high morbidity and mortality. Even with antibiotic treatment, poor clinical outcomes such as 10-20% patient death and 5-10% relapse persist due to problems with current care. Meropenem is the first line of defense against melioidosis, but is currently only available as an IV infusion. To overcome the challenges of systemic antibiotic delivery, a previously validated macromolecular inhalable prodrug delivery platform has been employed utilizing a novel meropenem prodrug monomer with hydrolysable phenolic ester linkage. Two polymers were synthesized via RAFT: a copolymer of meropenem and a mannose receptor targeting ligand to enhance cellular uptake, and a terpolymer of meropenem, ciprofloxacin, and mannose to investigate drug combination effects. Both polymer systems shows exceptional biocompatibility with no cytotoxicity observed to macrophage in culture. The copolymer exhibits good efficacy against the model bacterium *B. thailandensis* in a RAW 264.7 cell infection coculture assay, similar to that of a mannose-ciprofloxacin polymer previously reported. The terpolymer however, shows excellent bactericidal efficacy in the coculture assay, outperforming the single antibiotic polymers, indicating synergistic activity between ciprofloxacin and meropenem. These data provide promising results in the fight against pulmonary melioidosis and pointing towards combination therapies for future improvements.

2.2 INTRODUCTION

Burkholderia pseudomallei is the causative agents of Melioidosis, a bacterial infection with a mortality rate between 10-20% for treated, uncomplicated cases and as high as 40-80% when untreated, depending on disease severity and whether sepsis occurs [10, 11]. Much of the lethality of this disease is due to the ability of *B. pseudomallei* to reside within the alveolar macrophage following inhalation, where bacteria evade the immune system and become difficult to combat with traditional antibiotic therapies. Furthermore, this bacterium is aerosolizable and easily weaponized for use in bio-warfare; as such the DHHS, CDC, and USDA consider *B. pseudomallei* a tier 1 agent [29]. Current care is limited, requiring weeks of high dose intravenous or oral antibiotic delivery, and still results in a 5-10% disease relapse rate [12]. Poor treatment outcomes are due to problems with systemic antibiotic delivery such as poor drug bioavailability within the lungs, suboptimal pharmacokinetics, and undesirable off-target effects [41, 42]. As a result, there is great need for better drug delivery systems to combat pulmonary intracellular infections such as Melioidosis.

These challenges may be well addressed through development of inhalable polymeric prodrug delivery systems that could be administered directly to the site of infection thereby reducing the required antibiotic dose, eliminating off-target side effects and preventing development of antibiotic resistance, as well as allowing for controlled drug release and pharmacokinetic tailoring [57, 61, 63]. Additionally a dried powder, inhalable platform offers the advantages of being more rapidly employed in the event of a bioterrorist threat compared to traditional intravenous or oral delivery, and high drug stability without refrigeration would allow soldiers in the field to have treatment at the ready in the event of a bioterrorist attack [76, 77]. Many liposomal formulations have been developed to address some of the delivery challenges

associated with systemic antibiotic delivery, but with limited clinical translation. While liposomal systems can be administered directly to the lungs and enhance the stability and pharmacokinetics of antibiotics over systemic delivery, they're prone to low drug encapsulation efficiencies, often have burst release profiles, suffer from rapid clearance, and can require complex synthesis/formulation strategies making upscale manufacturing challenging [78-81]. Polymeric prodrug systems however, provide increased drug loading without the formulation complications leading to better manufacturability. Additionally, prodrug linkages can be tailored for more optimal drug release kinetics often at the specific disease target [57, 61, 63].

Previously, ciprofloxacin prodrug monomers were developed and copolymerized with polyethylene glycol methacrylate that demonstrated controllable near first-order release kinetics and promising efficacy and low toxicity in vitro [71]. These aerosolizable polymers were later shown to enhance treatment efficacy in a lethal murine Tularemia model, prolonging survival in 70% of treated mice to the experimental endpoint compared to untreated mice with 0% survival [72]. This work laid the foundation of the drugamer platform for inhalable antibiotic delivery for the treatment of intracellular pulmonary infections.

While ciprofloxacin had been previously modified as a polymerizable prodrug monomer [71, 82, 83], and has clinical use in the treatment of Tularemia, it is not a drug of choice in the treatment of Melioidosis. Meropenem is the drug of choice for clinicians in the treatment of severe Melioidosis. Treatment involves weeks of intravenous delivery within a hospital setting, as meropenem is not currently available in any other format [12, 13]. Here, we report the development of a novel meropenem prodrug monomer containing a hydrolysable phenolic ester linkage and the in vitro activity of two novel polymers synthesized via RAFT: a copolymer

comprised of the meropenem prodrug monomer and a mannose receptor targeting co-monomer and a terpolymer containing meropenem, ciprofloxacin, and the mannose-targeting ligand. The mannose monomer was employed for its ability to enhance drug-loading, biocompatibility, and improve cellular internalization via receptor-mediated endocytosis [84-86]. Analysis shows excellent biocompatibility for both polymers with no cytotoxicity to murine macrophage in culture. The copolymer exhibited good efficacy against the model bacterium *B. thailandensis* in a RAW 264.7 cell infection coculture assay similar to a previously reported copolymer containing ciprofloxacin and meropenem. The terpolymer, however, shows excellent bactericidal efficacy in the coculture assay outperforming both of the single antibiotic polymers, indicating possible synergy between these two antibiotics; one a beta-lactam that hinders bacterial cell wall synthesis, the other a fluoroquinolone that targets DNA gyrase activity [87]. These are promising data towards improved treatment of pulmonary melioidosis and suggest that combination therapies may be a more optimal treatment of intracellular pulmonary infections to overcome previous delivery challenges as well as reduce the dosage of antibiotics potentially slowing the development of antibiotic resistance.

2.3 Materials & Methods

2.3.1 **Materials**

All chemicals and materials were purchased from Sigma-Aldrich (St. Louis, MO) unless specified otherwise. Spectra/Por regenerated cellulose dialysis membranes (6-8 kDA cutoff) where obtained from Fisher Scientific (Bothel, WA). G-25 prepacked PD10 columns were purchased from GE Life Sciences (Issaquah, WA). All Bacteria stocks were provided by the Eoin West and Shawn Skerrett labs at Harborview Medical Center (Seattle, WA). RAW 264.7 cells were purchased from ATCC (Manassas, VA). MTS 96-cell titer viability reagents were

purchased from Promega (Madison, WI). All mammalian cell culture media, supplements, and PBS were purchased from Gibco (Fisher Scientific, Bothel, WA).

2.3.2 **Synthesis of meropenem carbamate methacrylate (MCM) prodrug monomer**

*Butanoic acid, 4-[(4-hydroxymethylphenyl]-4-oxo, 1-(2-methacryloyloxy)ethyl ester [**Scheme 2.1**, #3]*

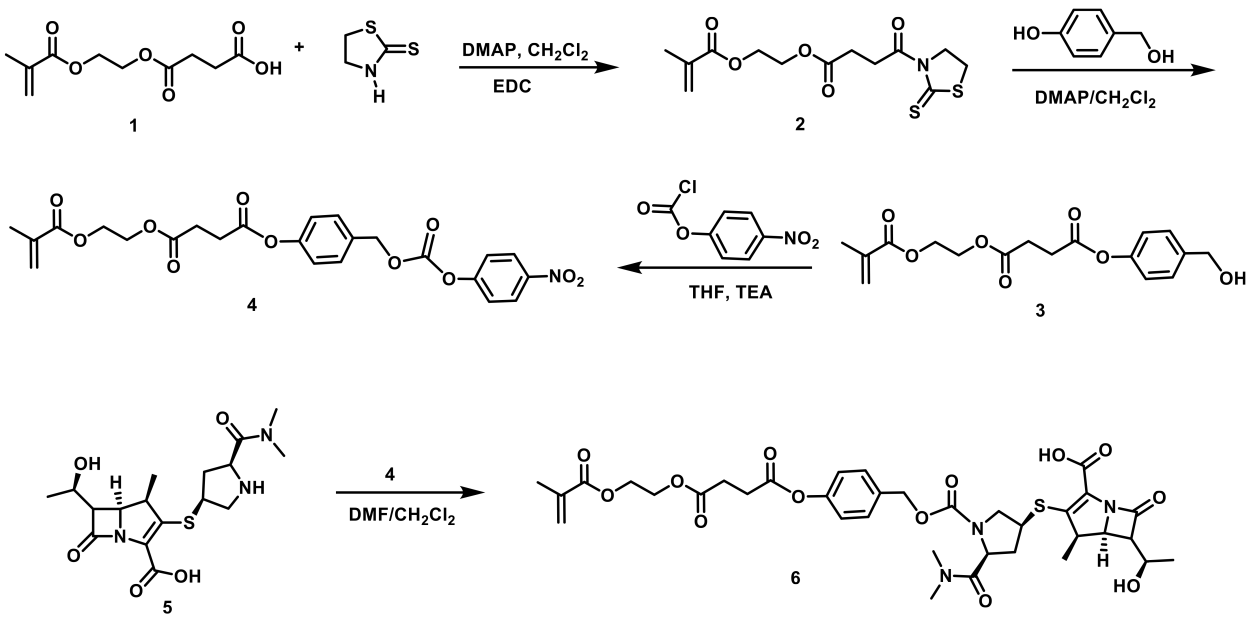

Scheme 2.1: Synthesis Scheme for the meropenem carbamate methacrylate (MCM) prodrug monomer

A mixture of mono-2-(methacryloyloxy)ethyl succinate (SMA, #1) (11.5 g, 50 mmol), 2-mercaptothioazoline (5.95 g, 50 mmol) and N,N-dimethylpyridin-4-amine (6.1 g, 50 mmol) in 250 mL of CH_2Cl_2 was treated with N-(3-dimethylaminopropyl)-N'-ethylcarbodimide hydrochloride (10 g, 52 mmol) at 0 °C. After 30 min, at 0 °C, the reaction mixture was stirred at room temperature for 8 h. CH_2Cl_2 was evaporated and the oily residue obtained was stirred with 100 mL of diethyl ether for 30 min. The ether layer containing the activated ester was collected by decanting. This process was repeated two more times. All the ether layers were combined, evaporated, and dried under high vacuum to yield product #2. To a solution of product #2 and

N,N-dimethylpyridin-4-amine (6.1 g, 50 mmol) in 350 mL was slowly added 4-hydroxybenzyl alcohol (9.3 g, 75 mmol) in 100 mL of $CHCl_3$ at 0 °C over 30 min. After 20 min at 0 °C, the reaction mixture was stirred at RT for 16 hrs. The solution was washed with 1N HCl (3×100 mL), 30% aqueous acetic acid (3×100 mL), and then with warm water (40 °C, 3×100 mL). The organic phase was dried over Na_2SO_4 and concentrated. The crude product was purified by silica gel column chromatography using 4% methanol in chloroform to afford compound #3. Yield 12.7 g (75.6 %)

*Meropenem carbamate monomer [**Scheme 2.1** (#6)]*

To an ice cooled solution of product #3 (6.73 g, 20 mmol) and trimethylamine (3.6 mL, 26 mmol) in 70 mL of tetrahydrofuran, was added p-nitrophenyl chloroformate (4.84 g, 24 mmol) pre-dissolved in 70 mL tetrahydrofuran over 30 min. After 30 min, the reaction mixture was slowly warmed to room temperature and stirred for 18 hrs. Triethylammonium hydrochloride formed was filtered off and the filtrate was concentrated. The crude product was purified by silica gel column chromatography using 33% ethyl acetate in n-hexane to obtain product #4. Yield = 8.21 g (81.9 %).

Meropenem (#5, 767 mg, 2.0 mmol) in 2 mL DMSO was treated with p-nitro phenyl activated carbonate (#4, 1.2 g, 2.4 mmol) pre-dissolved in 8 mL CH_2Cl_2. After stirring at room temperature for 20 hrs, the reaction mixture was precipitated in diethyl ether. The side product p-nitrophenol was successfully removed by five ether precipitations. Product was dried under high vacuum for 24 hrs to yield meropenem carbamate methacrylate monomer (MCM, #6). Yield = 1.22 g (81.8 %).

2.3.3 **Synthesis of ciprofloxacin tyramine methacrylate (CTM) prodrug monomer**

butanoic acid, 4-[(4-hydroxyphenyl)ethylamino]-4-oxo, 1-(2-methacryloyloxy)ethyl ester

To an ice cold solution of mono-2-(methacryloyloxy)ethyl succinate (9.2 g, 40 mmol) in 150 mL CH_2Cl_2, were added *N*-hydroxysuccinimide (4.72 g, 41 mmol) and *N*-*N*′-dicyclohexylcarbodimide (9.06 g, 44 mmol). After 15 min, the ice bath was removed and the reaction mixture was stirred at room temperature for 16 hrs. The byproduct dicyclohexylurea was filtered off, and the filtrate was concentrated to 40 mL by evaporating the solvent under reduced pressure. This solution containing the activated NHS ester was directly added to (6.85 g, 50 mmol) of 4-(aminoethyl)phenol pre-dissolved in 30 mL *N*,*N*-dimethylformamide, followed by 13.94 mL (0.1 mol) trimethylamine. After stirring for 6 hrs at RT, the reaction mixture was diluted with 200 mL CH_2Cl_2, and washed with water (2x 100 mL). The organic layer was dried over anhydrous sodium sulfate and concentrated under reduced pressure. The thick residue obtained was treated with 100 mL diethyl ether, and vigorously stirred for 15 min. Then 75 mL hexane was added, and again stirred well for 10 min. The solvent was carefully decanted and the process was repeated one more time. The product obtained was further purified by flash silica gel column chromatography using 5% methanol in chloroform. Overall yield for two steps: 11.2 g (80.1 %).

7-(4-(tert-Butoxycarbonyl)piperazin-1-yl)-1-cyclopropyl-6-fluoro-4-oxo-1,4-dihydroquionoline-3-carboxylic acid

To (20 g, 60 mmol) of ciprofloxacin in 350 mL of dioxane:water (1:1) was added 90 mL 1N NaOH, followed by (20 g, 91.6 mmol) of di-tert-butyl dicarbonate. The reaction mixture was stirred at room temperature for 17 hrs. The white precipitate obtained was filtered, washed with

water and then with acetone. The product was dried under high vacuum overnight. Yield = 25.14 g (96.5 %).

Boc protected ciprofloxacin tyramine methacrylate (CTM)

Boc protected ciprofloxacin (4.3 g, 10 mmol) and N,N-dimethylpyridin-4-amine (DMAP) (1.22 g, 10 mmol) were taken in 350 mL of CH_2Cl_2 and cooled to 4 °C. To this solution, N,N,N',N'-tetramethyl-O-(1*H*-benzotriazol-1-yl)uronium hexafluorophosphate (HBTU) (9.48 g, 25 mmol) was added, followed by N,N-diisopropylethylamine (7.0 mL, 40 mmol). After 10 min at 4 °C, the reaction mixture was stirred at RT for 30 min, and then cooled back to 4 °C. Phenolic monomer (3.49 g, 10 mmol) was introduced and the reaction was continuously stirred at 4 °C for 20 min, and then at RT for 16 hrs. The reaction mixture was filtered and the filtrate was washed with water (150 mL) and brine (150 mL). The organic phase was dried over anhydrous sodium sulfate and the solvent was evaporated under reduced pressure. The residue was precipitated in diethyl ether, and then purified by silica gel column chromatography using 30 % tetrahydrofuran in chloroform containing 0.1 % triethylamine. Yield = 5.76 g (75.5 %).

Synthesis of ciprofloxacin tyramine methacrylate (CTM)

BocCTM (2.29 g, 3 mmol) was treated with 25% trifluoroacetic acid in CH_2Cl_2 (60mL) at 4 °C, and the resulting solution was stirred at 4 °C for 5 min, and then at RT for 2 hrs. After evaporating solvent under reduced pressure, oily crude product was triturated with diethyl ether and the insoluble residue was dried under high vacuum to afford CTM. Yield = 2.31 g (99.1%).

2.3.4 **Synthesis of mannose ethyl methacrylate (MEM) targeting monomer**

1,2,3,4,6-Penta-O-acetyl-D-mannopyranose

D-Mannose (20.0 g, 111 mmol) was slowly added (in 10 portions) to a solution of Iodine (1.12 g, 4.41 mmol) in 100 mL Ac_2O at 0 °C under nitrogen atmosphere. After stirring for 30 min at 0 °C and an additional 16 hrs at RT, the reaction mixture was diluted with 150 mL CH_2Cl_2 and washed with a cold saturated aqueous solution of $Na_2S_2O_3$ (3x 100 mL), then with saturated aqueous solution of $NaHCO_3$ (5x 125 mL). The organic layer was finally washed with water (2x 100 mL), dried over Na_2SO_4 and evaporated under reduced pressure to afford the pentaacetate. The product was dried under high vacuum for 48 hrs and used for the next step without further purification.

2-(α-D-mannosyloxy)ethyl methacrylate

To a solution of α-D-mannose pentaacetate (9.0 g, 23.05 mmol) and 2-hydroxyethyl methacrylate (4.5 g, 34.58 mmol) in 40 mL anhydrous CH_2Cl_2 was added molecular sieves 4Å (5 g). After 30 min at RT, the mixture was cooled to 0 °C and BF_3Et_2O (20 ml, 159.24 mmol) was added. After stirring for 30 min at 0 °C and an additional 20 hrs at RT, the reaction mixture was diluted with 100 mL CH_2Cl_2. The resulting solution was washed with deionized water (1x 100 mL), saturated aqueous solution of $NaHCO_3$ (3x 100 mL) and again with deionized water (2x 100 mL). The organic layer was treated with dibutylhydroxytoluene (BHT, inhibitor, 20 mg) and dried over Na_2SO_4. The solvent was removed under reduced pressure to yield crude 2-(2',3',4',6'-tetra-*O*-acetyl-α-D-mannosyloxy)ethyl methacrylate. This crude product in 40 mL MeOH was treated with K_2CO_3 (2.0 g, 14.47 mmol) and stirred for 10 min. The reaction was neutralized by filtering into a flask containing Amberlite® IR120 hydrogen form resin (10 g), and the mixture was stirred for 5 min. The resin was removed via filtration and the solvent was subsequently removed under reduced pressure. The resulting sticky residue was purified by silica gel column chromatography using 12% MeOH in $CHCl_3$ as eluent. The oily product obtained

after column chromatography was dissolved in 6 mL MeOH and precipitated in 100 mL ether to yield monomer 4. Yield = 1.9 g.

All synthesized monomers were monitored throughout synthesis via thin layer chromatography to assess the progress of the reaction in each step. Synthesized monomers were purified either by flash column chromatography or precipitation techniques. Purity of all the materials was validated by ^{1}H NMR spectroscopy (Bruker Avance spectrometers 300 MHz or 500 MHz) and electron spray ionization mass spectrometry (ESI-MS) (Bruker Esquire ion trap mass spectrometer integrated with liquid chromatography).

2.3.5 RAFT polymerization of poly(MEM$_{co}$MCM), poly(MEM$_{co}$CTM), and poly(MEM$_{co}$MCM$_{co}$CTM)

All polymer synthesis was conducted using the reversible addition-chain transfer (RAFT) technique [68], with 4-((((2-Carboxyethyl)thio)carbonothioyl)thio)-4-cyanopentanoic acid (CCC) and 2,2′-Azobis(4-methoxy-2,4-dimethylvaleronitrile) (V70 in dioxane) as the RAFT chain transfer agent (CTA) and initiator, respectively. All polymers were synthesized with a molar feed ratio of 2:1 Mannose:prodrug, with the terpolymer containing equal mole parts ciprofloxacin and meropenem prodrugs. All polymerizations were conducted with an initial monomer $[M]_o$:$[CTA]_o$:$[I]_o$ ratio was 50:1:0.1 at an initial overall monomer concentration of 25 % m/v in dimethyl sulfoxide. Specific masses and volumes used are presented in **Table 2.1**. Polymerization reactions were combined in 100 mL round bottom flasks and septa sealed, then purged of O_2 under nitrogen for 30 min. Polymerization vials were then transferred to a preheated water bath and allowed to polymerize for 24 hours at 30 °C. After polymerization, reactions were precipitated with ice-cold diethyl ether 3x, vortexing and then centrifuging at 4200 rpm for 5 min, each. The final ether wash was poured off and the resultant polymers were

diluted in 0.5M phosphate buffer, pH 7.4 and dialyzed against deionized water at 5 °C for 24 hours. Dialyzed polymers were then dried by lyophilization, dissolved in deionized water, and further purified by filtration through a PD10 column. The final filtrates were lyophilized and stored at 4 °C. The final polymer molecular weights and Đ were measured by gel permeation chromatography (GPC) and polymer molar compositions were evaluated by ^{1}H NMR in $CDCl_3$.

2.3.6 **Drug Release Kinetic Analysis via HPLC**

Polymers were dissolved in human serum (Sigma) at 36 mg/mL and stored at 37°C. Samples were pulled, 200 µL each at T=0, 1, 3, 5, 7, and 10 days. 100% release was evaluated from polymer samples prepared at 6 mg/mL in either 100% H_2SO_4 (acidic conditions) or 0.1N NaOH (basic conditions), and stored at room temperature for 48 hours. All samples were stored at -80°C until ready for processing and analysis. On day of analysis, all samples were thawed on ice. Protein precipitation was conducted by adding 400 µL of Acetonitrile, vortexing 10s,

Table 2.1: RAFT polymerization reagent values used for the synthesis of poly(MEM$_{co}$MCM), poly(MEM$_{co}$MCM$_{co}$CTM), and poly(MEM$_{co}$CTM).

poly(MEMcoMCM)		
m MCM	0.333	g
m MEM	0.666	g
n MCM	0.0004465	mol
n MEM	0.002278637	mol
n CCC	5.45027E-05	mol
n V70	5.45027E-06	mol
m CCC	16.75414428	mg
m V70	1.680864703	mg
V CCC ST	0.990609677	mL
V V70 ST	0.099060968	mL
V DMSO	2.906329355	mL
Total Volume	3.996	mL

Poly(MEMcoMCMcoCTM)		
m MCM	0.1665	g
n MCM	0.00022325	mol
n CTM	0.00022325	mol
m CTM	0.170275161	g
m MEM	0.673550322	g
n MEM	0.002304469	mol
n CCC	5.50194E-05	mol
n V70	5.50194E-06	mol
m CCC	16.91296246	mg
m V70	1.696798186	mg
V CCC ST	1	mL
V V70 ST	0.1	mL
V DMSO	2.941301931	mL
Total Volume	4.041301931	mL

Poly(MEMcoCTM)		
m CTM	0.333	g
m MEM	0.666	g
n CTM	0.000436601	mol
n MEM	0.002278637	mol
n CCC	5.43048E-05	mol
n V70	5.43048E-06	mol
m CCC	16.69328317	mg
m V70	1.674758793	mg
V CCC ST	0.098701119	mL
V V70 ST	0.098701119	mL
V DMSO	3.798597762	mL
Total Volume	3.996	mL

followed by centrifugation at 4500rpm for 5 min. 100 μL of supernatant was then mixed with 900 μL deionized water and samples were put on ice until ready for HPLC analysis. HPLC analysis was conducted as previously described [88] with a few changes to the gradient. Analysis was carried out using an Agilent 1260 Quaternary HPLC Pump, Agilent 1260 Infinity Standard Automatic Sampler, Agilent 1260 Infinity Programmable Absorbance Detector, and Agilent ChemStation software (Palo Alto, CA). Analytes were separated using a Zorbax RX-C18 analytical column (4.6 x 150 mm; 5 μm). Mobile phase (A) 0.2% phosphoric acid and (B) acetonitrile were run at a flow rate of 1 mL/min over the following gradient: Starting at 5% (B) for 1 min, a linear increase to 15% (B) in 1.5min, increased to 70% (B) in 11min, back to 5% (B) in 30sec, and run at 5% (B) for 4 min to re-equilibrate the column. UV monitoring was conducted at 280 nm (ciprofloxacin and polymer backbone) and 304 nm (meropenem).

2.3.7 **In vitro Cytotoxicity Analysis**

RAW 264.7 cells were seeded at a density of 50,000 cells/well in 100 μL cDMEM (10% FBS, 1% pen/strep) into 96 well plates and incubated at 37°C with 5% CO_2 for 20 hours. Just prior to treatment polymers and free drug were dissolved (separately) in warmed cDMEM and sterile filtered (0.22μm). After 20 hours incubation, poly($MEM_{co}MCM$), poly($MEM_{co}CTM$), poly($MEM_{co}MCM_{co}CTM$), and free Meropenem were added to cells at concentrations of [10-4.88E-3 mg/mL polymer, 1-4.88E-4 mg/mL free Meropenem], then incubated for 24 hours. After incubation, cell media was removed and cells were gently washed with 100 μl of 1x PBS prior to addition of MTS reagent in phenol-free DMEM according to manufacturer's protocol (Promega). Cells were incubated in MTS reagent for 2 hours and absorbance was measured at 490nm on a Tecan plate reader. Data was corrected for background (negative control, media only) and plotted as percent viability after normalizing to the positive controls (untreated cells).

2.3.8 **In vitro Co-culture, Intracellular Infection Efficacy Analysis**

As described and validated previously [71], RAW 264.7 cells were seeded at a density of 500,000 cells/mL into 48-well plates in 300 μL antibiotic free DMEM + 10% FBS, and incubated at 37°C with 5% CO2. After 18 hours, cells were infected with Burkholderia thailandensis at early log phase (OD600=0.2) at a multiplicity of infection of 5, then incubated for 1 hour. Following incubation, growth media was replaced with fresh DMEM containing 10% FBS and 250 μg/mL Kanamycin to kill any bacteria not internalized by the RAW cells, then incubated for another hour. Growth media was then replaced with fresh media containing varying concentrations of poly(MEM$_{co}$MCM), poly(MEM$_{co}$CTM), poly(MEM$_{co}$MCM$_{co}$CTM), free Meropenem, or free Ciprofloxacin. Treated cells were then incubated 22 additional hours. After incubation, cell media was aspirated, cells were washed three times with 1x PBS, and lysed with 100 uL of PBS + 0.1% Triton X-100. Duplicate well lysates were pooled by treatment, serially diluted, and plated onto triplicate LB agar plates at appropriate 10x dilutions, then incubated for 24 hours. When individual bacterial colonies were distinguishable (~ 24 hours), CFUs were counted. Data is represented as CFU/well vs. antibiotic dose. All polymers were all assumed to be 15 wt% antibiotic based on the theoretical wt%, calculation from monomer feed ratios and from previous, similar polymers [71].

2.3.9 **Drug Combination Analysis against *Burkholderia thailandensis***

A standard checkerboard assay was performed to collect drug combination data and the ED_{50} endpoint used to construct an isobologram, similarly to others [89-91]. A single colony of *Burkholderia thailandensis* was picked from a streak plate and grown in 5mL LB broth at 37°C at 200 RPM. After 24 hours, the culture was diluted in 50mL of fresh LB broth at a 1:100 ratio and grown to early log phase (OD_{600}=0.2 based on previous growth curves). Varying

concentrations of free Meropenem (2.5-1.2E-3 μg/mL) against varying concentrations of free Ciprofloxacin (8-3.9E-3 μg/mL) were added to a 96 well plate in 50uL LB broth. Bacteria were then added to each well at 1x106 cells/mL in LB. A control plate with each antibiotic alone and a positive (bacteria w/o treatment) and negative (LB broth only) control was also run. Plates were incubated for 24 hours at 37°C. After 24 hours, the OD_{600} was measured on a Tecan plate reader; the average OD_{600} was calculated from 5 reads per well after 2 sec of shacking. Data was collected from triplicate wells run on duplicate days. All data were corrected by subtracting the negative control (media only) and normalizing to positive control (bacteria w/o treatment). Growth curves were plotted as percent bacterial viability vs. the log of the antibiotic concentration. Curves were created in GraphPad Prism software and ED_{50} values (Effective dose to achieve 50% bactericidal activity) were calculated using nonlinear regression, inhibitory dose-response, log(inhibitor) vs. normalized response. Resultant ED_{50} values were plotted on an isobologram as drug pairs of (x,y) (ED_{50} of meropenem, ED_{50} of ciprofloxacin). Individual concentrations were selected for comparison between single drug treatment vs. combination drug treatment for evaluation of effects above and below the ED_{50} value for comparison with traditional isobologram analysis.

2.4 RESULTS & DISCUSSION

2.4.1 **RAFT polymerization and polymer characterization**

Scheme 2.2 illustrates the synthetic strategy for the copolymerization of mannose ethyl methacrylate (MEM) targeting co-monomer and meropenem prodrug monomer with phenyl ester

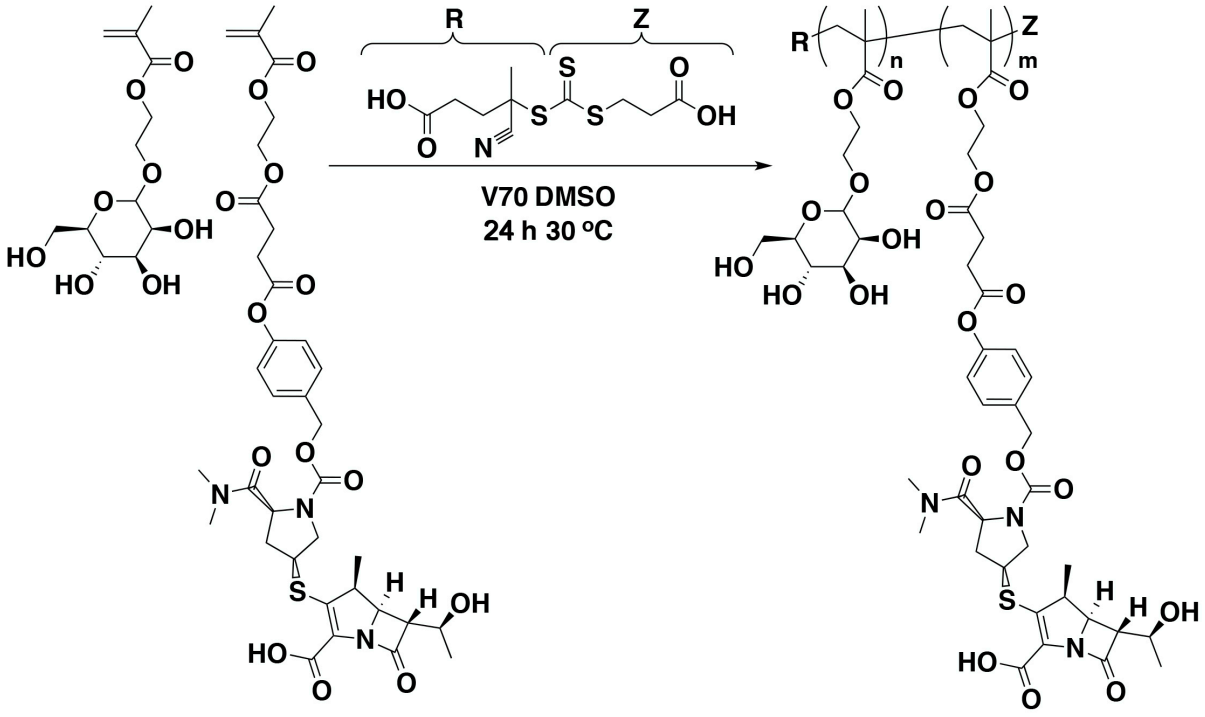

Scheme 2.2: Strategy for synthesis of poly(MEMcoMCM) via RAFT polymerization

hydrolysable linker (MCM), to produce poly(MEM$_{co}$MCM) linear copolymer via RAFT polymerization. A similar strategy was employed for the synthesis of poly(MEM$_{co}$CTM) and poly(MEM$_{co}$MCM$_{co}$CTM). The molar feed ratio of 2:1 mannose:prodrug was selected for high drug loading with optimal biocompatibility based on similar, previously reported polymers [71, 72]. Polymer compositions were estimated based on ^{1}H NMR [**Figure 2.1**], which was able to confirm polymer synthesis and quality purification.

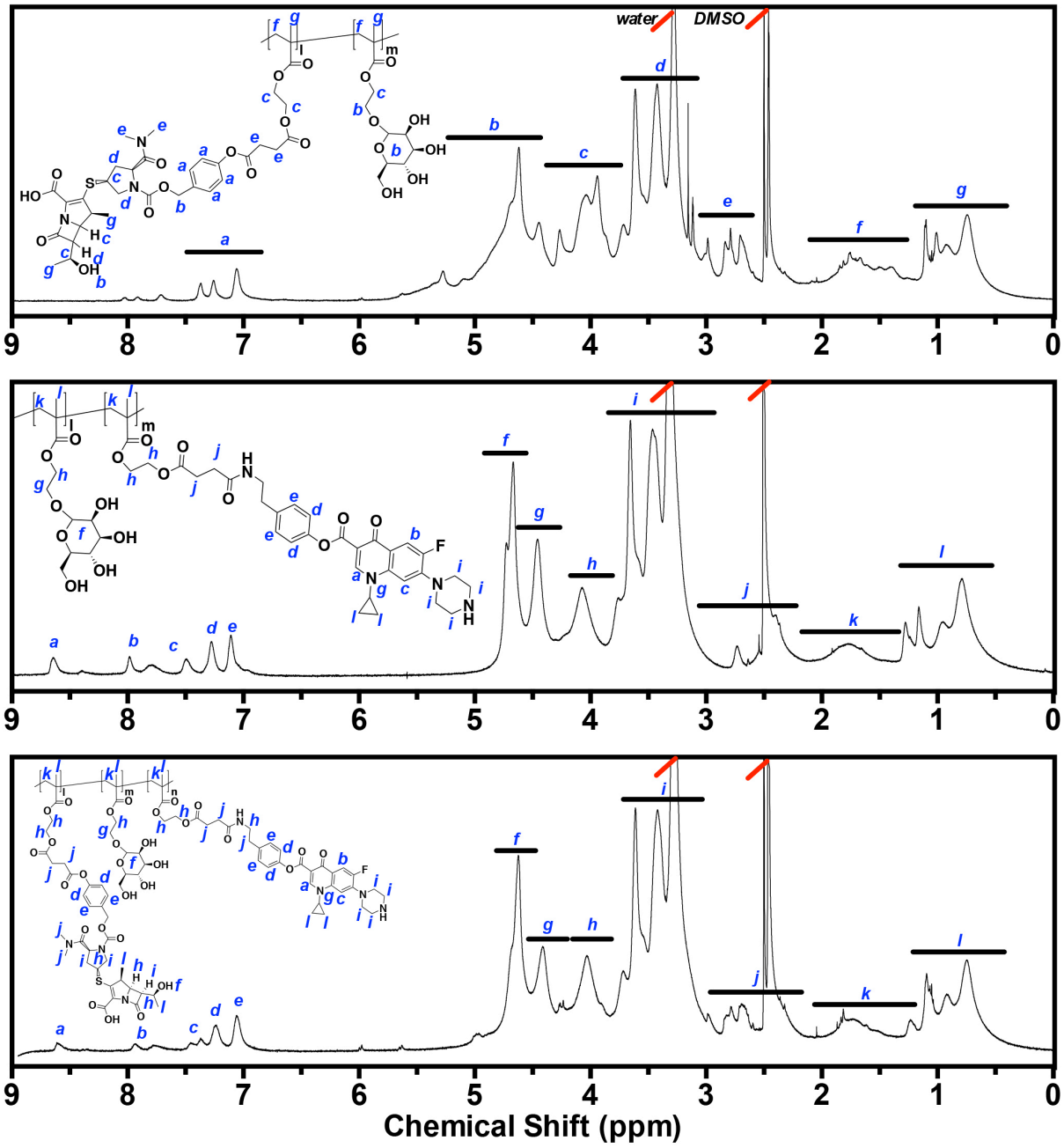

Figure 2.1: Polymer Characterization via ^{1}H-NMR. Chemical shifts for (top) poly(MEM$_{co}$MCM), (middle) poly(MEM$_{co}$CTM), and (bottom) poly(MEM$_{co}$MCM$_{co}$CTM)

However, due to the complexity of the polymers and resulting NMR spectra, precise composition and drug loading could only be estimated at the theoretical 15 wt.% antibiotic. An additional method must be employed to verify precise drug loading, likely via HPLC detection, calculation

of concentration based on standard curves, and confirmed by comparison to a sample 100% degraded in an appropriately selected acid or base (see the following drug release section).

2.4.2 **Drug Release Kinetics via HPLC: Challenges & Future Studies**

In order to understand the release kinetics of antibiotics from the polymer backbone, HPLC was employed to detect meropenem, meropenem degradation product, ciprofloxacin, and polymer, simultaneously. A method was adapted from Pinder et al. utilizing a mobile phase of 0.2% phosphoric acid against acetonitrile [88]. The method was evaluated using free meropenem dissolved at varying concentrations in deionized water or human serum as well as ciprofloxacin and a meropenem sample left at RT and allowed to degrade until no meropenem signal was detected. Meropenem, degraded meropenem, and ciprofloxacin were all detectable with unique peaks at 6.4, 5.8, and 7.6 minutes, respectively. Standard curves of meropenem in water [**Figure 2.2, top**] and human serum [**Figure 2.2, bottom**] were linear from 0.39-800 μg/mL and 3.125-800 μg/mL, respectively. It should be noted that higher concentrations were not evaluated, so this range simply defines the lower limit of detection. To evaluate antibiotic release from the polymer systems, poly(MEM$_{co}$MCM), poly(MEM$_{co}$CTM), and poly(MEM$_{co}$MCM$_{co}$CTM) were dissolved in human serum at 36 mg/mL, a T_0 time point was pulled, and samples were incubated at 37 °C. To determine 100% release, polymers were also dissolved separately in either H_2SO_4 or 0.1N NaOH and stored at RT for 48 hours to evaluate acidic vs, basic degradation. Time points were pulled from the incubating polymers (200 μL each) at days 1, 3, 5, 7, and 10. Samples were processed to remove proteins from the human serum by adding 2x the volume of HPLC grade acetonitrile (400 μL), vortexing, and centrifugation. Supernatant was then mixed with deionized water at 1:10 and samples were stored on ice until analyzed.

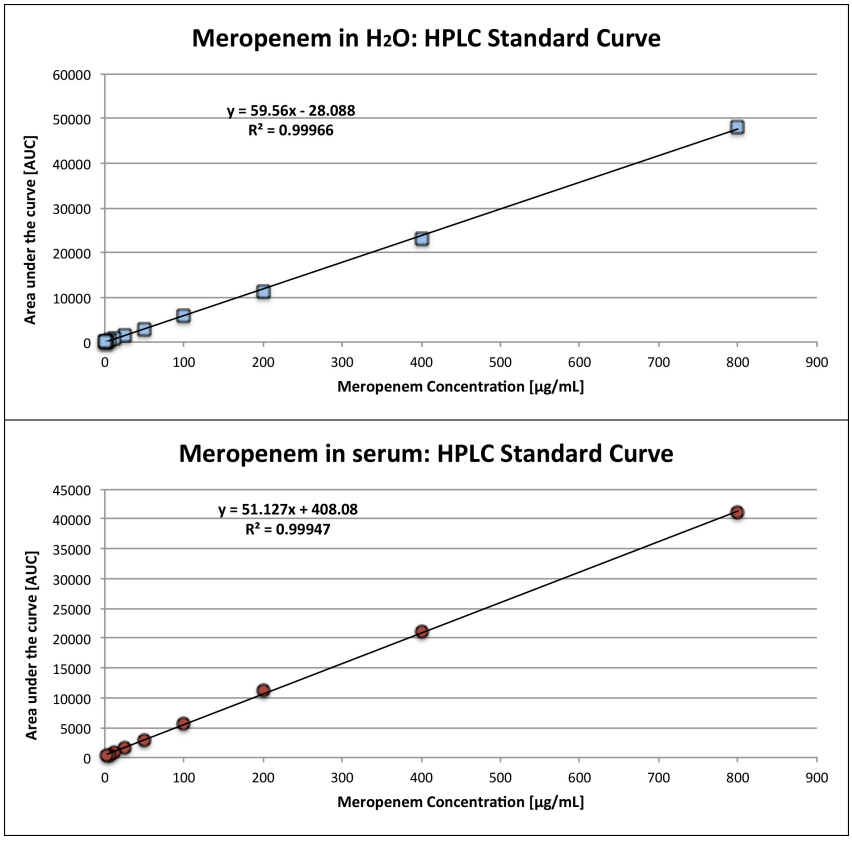

Figure 2.2: HPLC Meropenem Standard Curves prepared in (top) deionized water and (bottom) human serum.

Unfortunately, the 100% release samples of poly(MEM$_{co}$MCM) and poly(MEM$_{co}$MCM$_{co}$CTM) did not show either the meropenem peak or the meropenem degradation product peak. The poly(MEM$_{co}$MCM) also did not have the characteristic polymer peak, but was very similar to a blank run. The terpolymer did, however, have the characteristic ciprofloxacin and polymer backbone peaks without the meropenem. In the meropenem standard curves, a slight reduction in the AUC was observed when comparing the water prepared samples to the human serum samples and within the serum samples, no meropenem was detected at the lower concentrations (0.39-1.56 µg/mL) where meropenem was detectable in the water prepped samples. Combined with other observations discussed later, it's hypothesized that the meropenem may be interacting with the serum proteins to be removed during the protein

precipitation step and/or slow or obscure the meropenem release from the polymer. The lack of meropenem in the 100% samples is particularly confounding as meropenem is so readily degradable and the samples themselves turn yellow as free meropenem prepared in either water or serum does when left at room temperature to degrade. Why the 100% samples in both acidic and basic conditions should produce no detectable meropenem via HPLC suggests something else is happening, possibly during the sample preparation with acetonitrile. Additional studies are needed before drug release can be attempted again. Specifically, 1) meropenem retention needs to be evaluated before and after protein extraction, 2) Meropenem 100% release samples should be processed without acetonitrile, but instead by dilution with either the mobile phase, 0.2% phosphoric acid, or in deionized water to determine if the acetonitrile plays any role in the loss of meropenem, 3) If the acetonitrile plays no role in meropenem loss, as it shouldn't, the samples may need more than 48 hours to degrade or an alternative acid and base may need to be found in the literature, 4) It should be noted that previous drug release studies were under gentle rocking motion while polymers were incubating at 37 °C. That rocker was no longer in the incubator at the time of this study and could not be found. While not likely, it's possible the polymer required a bit of motion to prevent protein association and allow efficient hydrolysis of the prodrug linker. When the study is repeated, a rocker should be located and used.

In addition to troubleshooting the loss of meropenem problems, the observed meropenem, meropenem degradation product, ciprofloxacin, and polymer backbone HPLC peaks should be verified by collecting those peaks and running mass spectroscopy analysis to confirm expected masses of those product.

2.4.3 **In vitro cytotoxicity Analysis via MTS Assay**

To determine the biocompatibility of the polymer systems, an in vitro cytotoxicity assay was conducted in RAW 264.7 murine macrophage cells. Cells were seeded into 96-well plates and allowed to adhere for 18 hours before varying concentrations of poly($MEM_{co}MCM$), poly($MEM_{co}CTM$), poly($MEM_{co}MCM_{co}CTM$), and free meropenem were delivered. Once treated with polymer, cells were incubated for 24 hours prior to media removal and replacement with a tetrazoleum salt reagent (MTS). The colorimetric change of the MTS reagent was

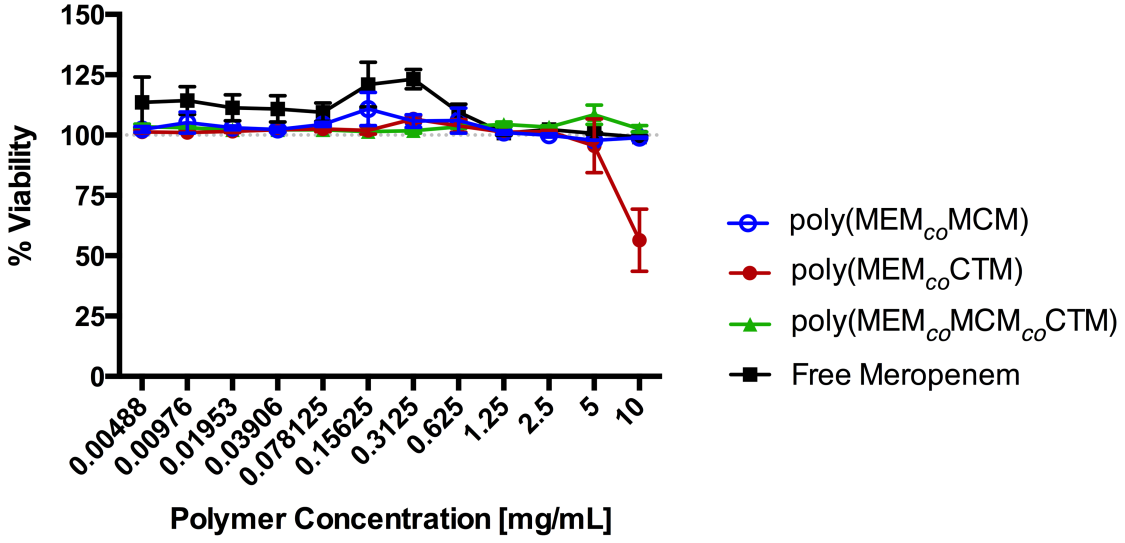

Figure 2.3: in vitro cytotoxicity analysis via MTS assay for poly(MEMcoMCM), poly(MEMcoCTM), poly(MEMcoMCMcoCTM), and free meropenem shows excellent biocompatibility for all polymers and free drug up to 5 mg/mL.

analyzed at 490nm on a plate reader and adjusted to remove the background (negative control, empty wells) and then normalized to healthy cells (positive control, untreated cells). No toxicity (100% viability) was observed for any of the polymers or free drug up to 5 mg/mL [**Figure 2.3**]. The poly($MEM_{co}CTM$) became somewhat toxic at 10 mg/mL (55% viability), while the other treatments remained completely nontoxic. This is likely due to the protonatability of the

ciprofloxacin and potential membrane association/destabilization that is not present with meropenem. This observation has not been shown to be physiologically relevant in vivo [73].

2.4.4 In vitro Bactericidal Efficacy via Coculture Mammalian Cell Infection Assay

To investigate the potential of these polymers to combat intracellular infection, their bactericidal efficacy against the model bacterium *B. thailandensis* was evaluated within RAW 264.7 cells as previously described [71]. The coculture assay captured the full dose response for all three polymers as well as free meropenem and ciprofloxacin [**Figure 2.4**]. As expected, ciprofloxacin had the lowest MIC near 10 μg/mL, consistent with previous data and published

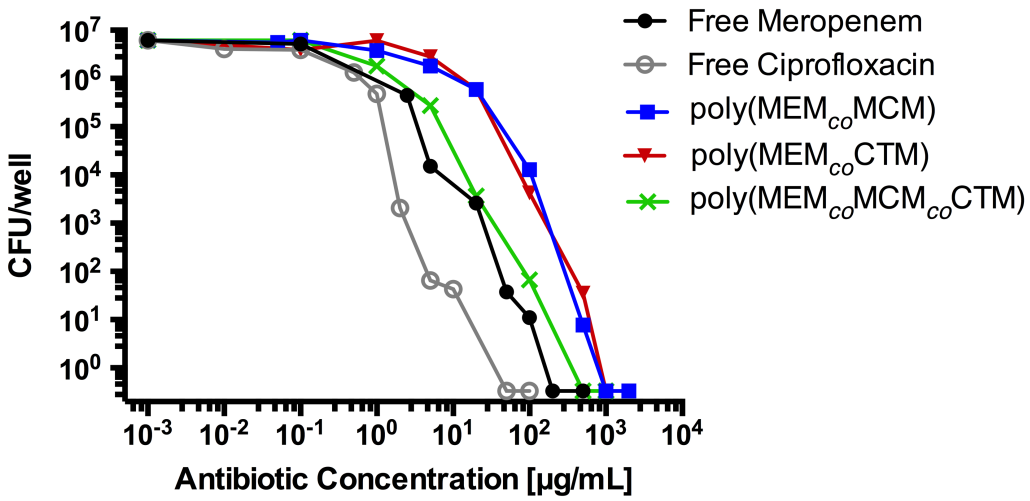

Figure 2.4: in vitro mammalian cell intracellular infection coculture assay results show the full dose response curves for free antibiotics vs. polymeric carriers against the model bacterium *B. thailandensis*.

values [37, 92]. Free meropenem, while more efficacious against Burkholderia in vivo compared to ciprofloxacin [10, 13], had a higher MIC value in this assay near 100 μg/mL. This difference is likely due to poor intracellular accumulation of beta-lactams within mammalian cells compared to good accumulation of fluoroquinolones; the mechanisms of which are still under investigation [93, 94]. Interestingly, the poly(MEM$_{co}$MCM) and poly(MEM$_{co}$CTM) had near identical dose

response curves and MIC values near 500 μg/mL. In the absence of drug release kinetics, there may be two explanations for this effect. The first, and least likely, is that the meropenem is releasing at a faster rate than the ciprofloxacin from the polymer backbone making up the difference in intracellular accumulation of the free drugs. Without data, this possibility can't be ruled out, but is unlikely due to the similarities between the poly(MEM$_{co}$MCM) and

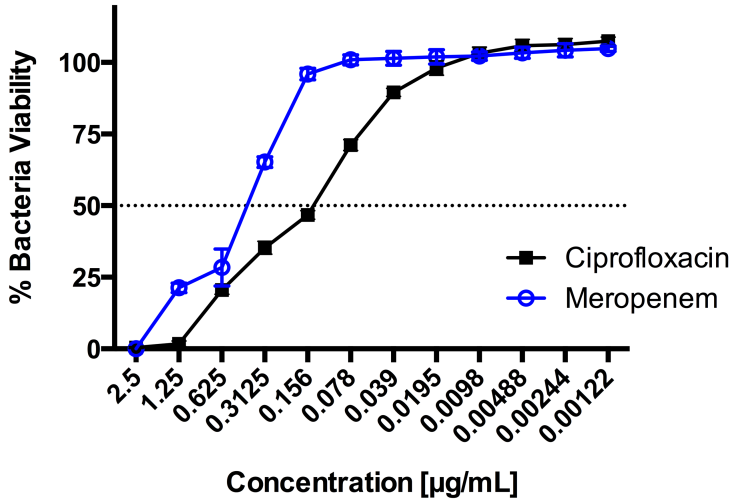

Figure 2.5: Bactericidal activity of free meropenem vs. ciprofloxacin in *B. thailandensis* planktonic assay shows ciprofloxacin has slightly improved activity (1 μg/mL MIC) in culture compared to meropenem (2.5 μg/mL MIC).

poly(MEM$_{co}$CTM) polymers and prodrug linkages. The second, and far more likely, possibility is that the mannose ligands are increasing the cellular uptake of both polymers, and the released drugs are in direct contact with the intracellular bacteria. An in vitro planktonic assay comparing the efficacy of free ciprofloxacin vs. meropenem against *B. thailandensis* alone revealed that ciprofloxacin slightly more bactericidal (1 μg/mL MIC) in culture against this model bacterium than is meropenem (2.5 μg/mL MIC) [**Figure 2.5**], in contrast to in the clinical setting against *B. pseudomallei*.

Finally, the terpolymer containing equal wt% meropenem and ciprofloxacin showed improved intracellular bactericidal activity over the single antibiotic polymer counterparts, with

an MIC more similar to free Meropenem near 100 μg/mL. This improvement in activity, despite the same amount of drug, indicates these two antibiotics aren't just additive in nature, but possibly synergistic. This result isn't unexpected given the differences in their mechanisms of action, with meropenem acting to prevent bacterial cell wall synthesis and ciprofloxacin inhibiting DNA gyrase activity [87].

2.4.5 **Antibiotic Combination Analysis in a *B. thailandensis* Planktonic Assay**

To investigate the bactericidal effects of ciprofloxacin and meropenem in combination against *B. thailandensis*, a standard checkerboard assay was performed for isobologram analysis. The assay was repeated in triplicate wells on duplicate days and the data presented separately in **Figure 2.6 [top]**. The region of the isobologram of high ciprofloxacin concentration to low meropenem concentration differs by day, appearing for one data set to show an additive effect and for the other day an antagonistic effect. Two additional processing techniques were applied to the data to attempt to clarify. For the first, all data for both days were combined and growth curves created. From those growth curves, ED_{50} values were determined and plotted [**Figure 2.6, middle**] as dose pairs. For the second, each data set was kept separate and ED_{50} values were determined, then the two ED_{50} dose pairs were averaged and plotted [**Figure 2.6, bottom**]. Without a third repeat of the checkerboard assay, it cannot be accurately determined what the true nature of the combination effect is using the ED_{50} endpoint as is traditional for isobologram analysis. When viewed together with the coculture assay data [**Figure 2.4**], the isobologram analysis is confounding. It's possible that because the ED_{50} values for each drug individually are so close, 0.5 μg/mL for meropenem and 0.55 μg/mL for ciprofloxacin, that even subtle

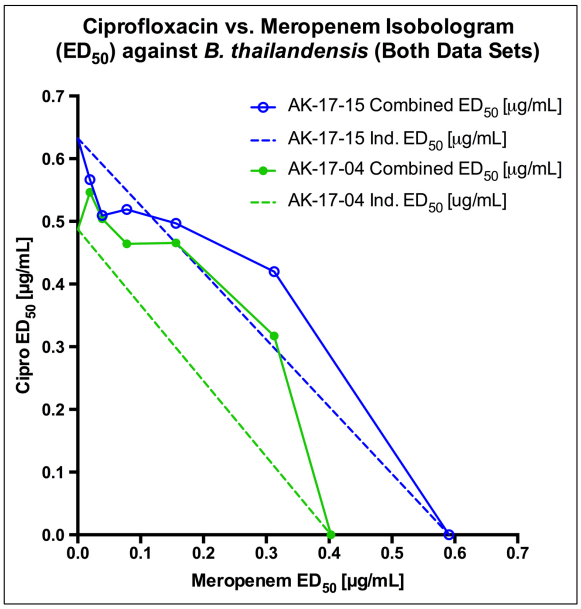

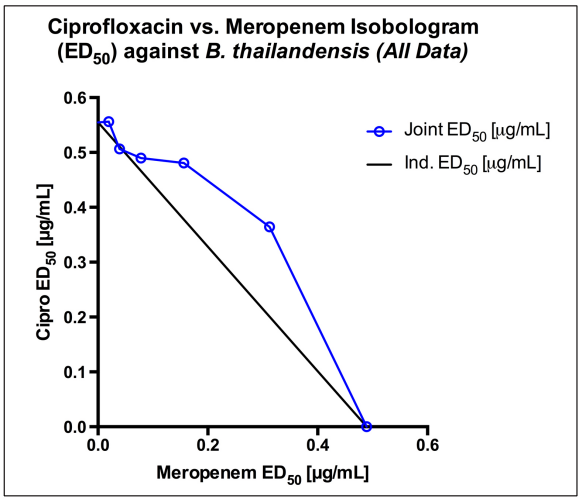

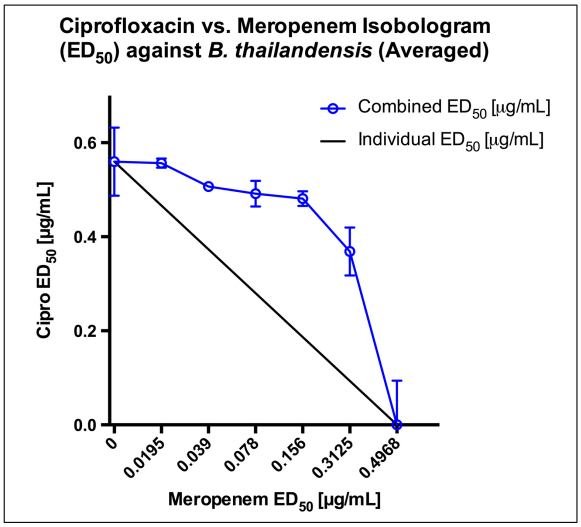

Figure 2.6: Isobologram analysis of checkerboard drug combination assay data. (top) duplicate day data presented separately, (middle) all data combined to create dose response curves from which ED_{50} values were calculated and then plotted, and (bottom) duplicate day data was kept separate for ED_{50} determination, then ED_{50} values were averaged and plotted. All plots indicate some degree of antagonism between meropenem and ciprofloxacin against *B. thailandensis* in planktonic assay.

fluctuation in technique or bacterial culture cause perceptible differences in the ED_{50} dose pairs for these drugs. It's also possible that the ED_{50} endpoint is inappropriate to capture the actual effect of meropenem in combination with ciprofloxacin against *B. thailandensis* and a different technique needs to be used, such as the Chou-Talalay method which does not rely on a single endpoint (like the ED_{50}) [95].

Finally, it could be the nature of the assay itself. Here, free meropenem and free ciprofloxacin are prepared in LB broth prior to addition of bacteria. Every effort is made so that the antibiotics are

prepared immediately prior to bacteria addition, but due to the nature of bacterial growth, the antibiotics often sit for 15-45 minutes at room temperature. There may be some interaction between the antibiotics due to the hydrophilicity of the meropenem and hydrophobicity of the ciprofloxacin that's causing an antagonistic effect in planktonic culture that is counter to the synergistic activity when the antibiotics are polymerized and kept separate until hydrolysis occurs.

Many reports on the combinatorial effects of meropenem and ciprofloxacin against various bacteria, including *Burkholderia cepacia*, indicate these two antibiotics are most often additive, sometimes synergistic, and very rarely antagonistic in combination [96, 97]. Because no previous study, to date, has investigated the combinatorial effects of meropenem and ciprofloxacin against either *B. thailandensis* or *B. pseudomallei*, and because different strains of the same bacteria can often behave differently, further study is needed to draw any definitive conclusions regarding the potential synergy between these antibiotics against these bacteria.

2.5 CONCLUSIONS

A novel hydrolysable meropenem prodrug monomer was successfully synthesized and copolymerized with a mannose targeting ligand to improve internalization into alveolar macrophage for the treatment of pulmonary melioidosis. A terpolymer containing mannose, meropenem, and ciprofloxacin was also presented as a first step towards combination antibiotic therapies utilizing the macromolecular inhalable prodrug format developed previously in the Stayton lab. These polymers have excellent biocompatibility in culture and show good efficacy against the intracellular *B. thailandensis* coculture infection model, with the terpolymer exhibiting exceptional efficacy particularly compared to free meropenem. While much additional work is needed, these results indicate the strong likelihood that these systems will be efficacious

at combating pulmonary melioidosis in vivo and provide a strong foundation for the development of other combination therapies utilizing this novel synthetic synthesis approach to overcome many of the challenges associated with both systemic antibiotic delivery and other nanoparticle drug encapsulation approaches.

2.6 ACKNOWLEDGEMENTS

This work was funded by the Defense Threat Reduction Agency (HDTRA1-13-0047) and a National Science Foundation Graduate Research Fellowship (DGE-10410000).

Chapter 3. FUTURE WORK

3.1 IN VIVO ANALYSIS

While the in vitro analysis looks promising, the assays are artificial and don't always translate to biocompatibility or efficacy in animal models and/or in humans. To truly evaluate the ability of these meropenem polymer systems to combat pulmonary melioidosis, in vivo analysis is critical. Preliminary in vivo toxicity results indicate some degree of inflammation to the lungs [Figure 4.1]. For these studies, 10 mice were be treated for three days, once per day with either 50 μL of PBS (n=5) or 40 mg/kg [**Figure 3.1, top**] or 20 mg/kg [**Figure 3.1, bottom**] of polymerized Meropenem within the poly($MEM_{co}MCM$) (n=5) (solubilized in PBS, sterile filtered 0.22 μm, and delivered in 50 μL). Mice were weighed before treatment each day and just prior to euthanasia. On day four, 24 hours after the third dosing, mice were euthanized by CO_2 asphyxia followed by exsanguination via heart puncture. Lungs were then lavaged with three repeat washes of 800 μL PBS and harvested. Harvested lungs were homogenized (LTH) in PBS with protease inhibitor and bronchoalveolar lavage fluid (BALF) was separated from lavaged cells by centrifugation. Lavaged cells were mounted on glass slides and stained via hemacolor for differential cell count. BALF and LTH were analyzed via ELISA for TNF-α levels. From these data, we can see that for the 40 mg/kg treatment group, their weight dropped by almost 20% over the dosing schedule and the neutrophil infiltration into the lungs was dramatically elevated near 70%, above that of even bleomycin induced lung fibrosis, which is reported at 30% neutrophil [98]. The lower dose of 20 mg/kg lessened the inflammatory response but did not eliminate it. Polymer treated mice exhibiting not quite 40% neutrophil infiltration and an average reduction in weight of 3% compared to control mice with a healthy 1-3% neutrophil

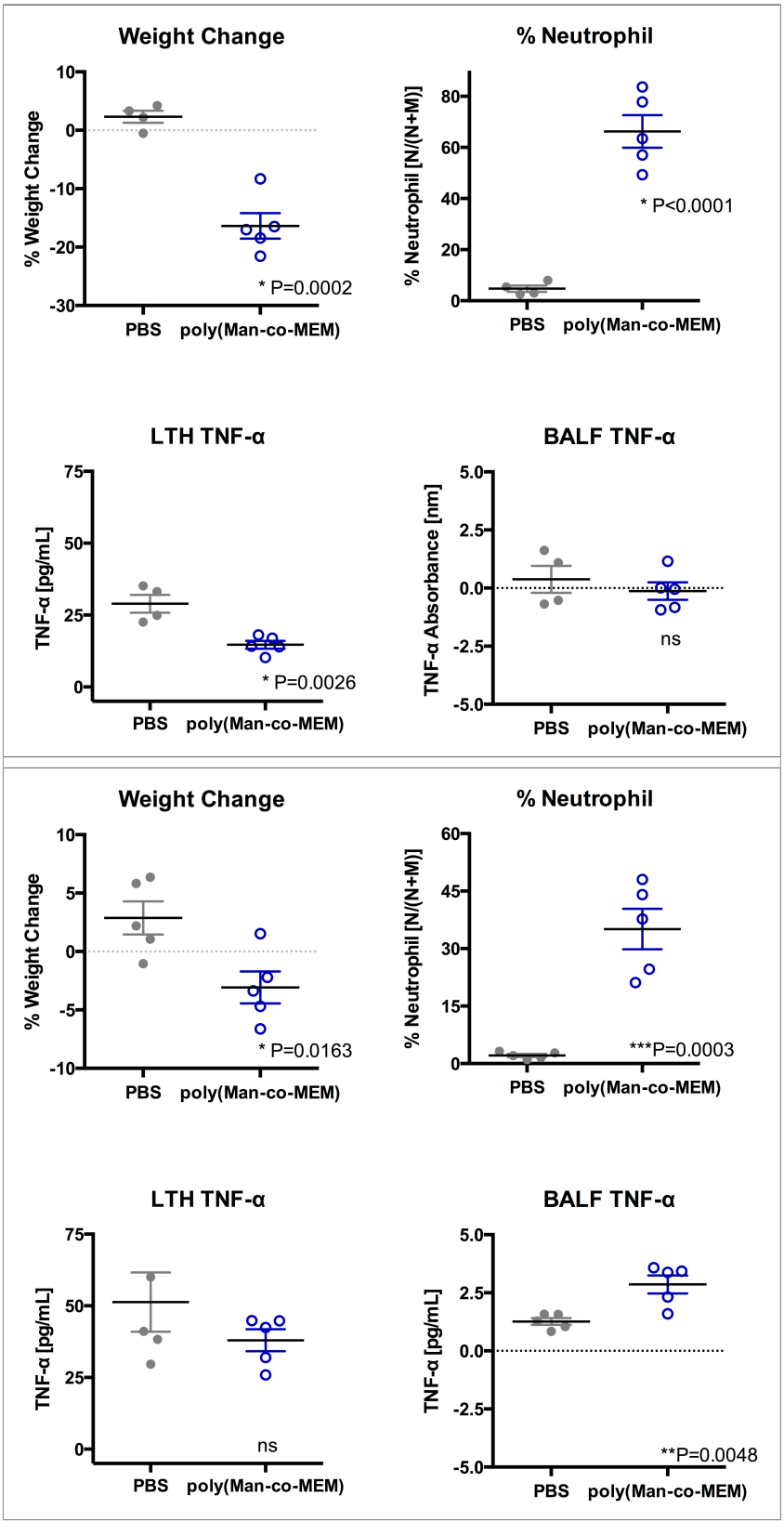

Figure 3.1: In vivo gross toxicity analysis of poly(MEM$_{co}$MCM) in black 6 mice, following 3 aerosolized, repeat doses, 1 every 24 hours of polymer in 50 µL PBS at a dose of (top) 144 mg/mL (40 mg/kg assuming 10% drug loading) polymerized meropenem, and (bottom) 43 mg/mL (20 mg/kg assuming 15 wt% drug loading) polymerized meropenem compared to PBS only control.

and slight weight gain overall.

These results were unexpected given the low toxicity observed with near identical polymer systems containing ciprofloxacin rather than meropenem [99], and the fact that meropenem is considered safe for systemic delivery, is hydrophilic, and has no readily protonatable side groups that might carry a positive charge in vivo. However, a recently

published study by Imani et al. looked at the concentration/toxicity relationships of some β-lactams by monitoring various toxicity markers in patients at St. Vincent's Hospital in Sydney Australia following antibiotic treatment. They found that meropenem carried a 50% risk of neurotoxicity at concentrations above just 0.0642 mg/mL and a 50% risk of nephrotoxicity at concentrations above 0.0445 mg/mL [100]. While this study did not evaluate any markers of lung toxicity or signs of inflammation, the low concentrations associated with a 50% risk of other types of toxicity indicate that the 20 mg/kg dose of meropenem in our studies (corresponding to 43 mg/mL) could very likely be responsible for the observed % neutrophil increase rather than the polymer itself. Additionally, in a case study published this year a woman treated with meropenem for a knee infection and 6 weeks later presented with pneumonia [101]. A lung lavage revealed an 89% eosinophil infiltration. Eosinophils are leukocytes that target parasites and modulate some allergic inflammatory responses. Neutrophils are the primary leukocyte responsible for bacteria and fungi destruction. These cell types are very similar in appearance and H&E stain, and without an eosinophil granule specific stain, they are indistinguishable to the untrained eye [102]. This is another piece of evidence suggesting that the meropenem itself is causing the observed toxicity in our studies.

Moving forward, a free meropenem control should be evaluated in vivo to determine the specific contribution of free drug to the observed toxicity. A dose escalation study could determine what the toxic dose threshold is and help guide future polymer studies. Doses below those suggested by the Imani study (<0.0445 mg/mL) and up to the 43 mg/mL concentration used for the 20 mg/kg toxicity study [**Figure 3.1, bottom**] should be evaluated to determine the window of safety. From that data, a third polymer toxicity study may be conducted or a reduced polymer dose could be selected for in vivo efficacy in the *B. thailandensis* mice infection model

in collaboration with the West lab at Harborview. Given the potency of free meropenem in vivo, it's quite possible the doses required for ciprofloxacin efficacy in vivo are higher than is necessary with meropenem, even given the similar MICs in vitro [**Figure 2.5**].

3.2 COMBINATION THERAPIES

The exceptional bactericidal activity of the terpolymer, poly(MEM$_{co}$MCM$_{co}$CTM) may be evidence of drug synergy between meropenem and ciprofloxacin given the degree of magnitude difference in it's dose response curve against B. thailandensis compared to the single antibiotic polymers, poly(MEM$_{co}$MCM) and poly(MEM$_{co}$CTM). To further investigate this potential, multiple studies are needed. A third repeat of the checkerboard/isobologram analysis could clear up the ambiguity of the current data set. However, it's also clear the very nature of the assay may be causing some of the discrepancies in observed activity between the free drug interactions in planktonic assay vs. the activity of the drugs from the polymer. A better study may be a similar approach but by combining the poly(MEMcoMCM) and the poly(MEMcoCTM) instead of free drug. In the event the polymers are protecting the antibiotics and preventing hydrophobic/hydrophilic interactions, this approach may be more revealing as to the actual activity of the drugs in combination within a polymer.

Additionally, in vivo studies for all three polymers should be conducted once the toxicity challenges are worked out, as mentioned above. The artificial nature of in vitro studies may be part of the problem between the conflicting drug combination study and the coculture assay data. Given the rise of antibiotic resistance, reducing antibiotic dosages by an order of magnitude could have a dramatic effect in slowing the development of more drug resistance bacterial strains.

BIBLIOGRAPHY

1. Organization WH. Top 10 Causes of Death. *Global Health Observatory (GHO) data*. 2015.
2. Lab P. Drug Nano-Carriers Marching towards Process Inensification. 2015.
3. Zaffiri L, Gardner J and Toledo-Pereyra LH. History of antibiotics. From salvarsan to cephalosporins. *Journal of investigative surgery : the official journal of the Academy of Surgical Research*. 2012;25:67-77.
4. Obama B. The National Action Plan for Combating Antibiotic-Resistant Bacteria. 2014.
5. Prevention CfDCa. Antibiotic Stewardship Statement for Antibiotic Guidelines. 2017.
6. Sjostedt A. Tularemia: History, epidemiology, pathogen physiology, and clinical manifestations. *Francisella Tularensis: Biology, Pathogenicity, Epidemiology, and Biodefense*. 2007;1105:1-29.
7. Ellis J, Oyston PCF, Green M and Titball RW. Tularemia. *Clinical Microbiology Reviews*. 2002;15:631-+.
8. Oyston PCF, Sjostedt A and Titball RW. Tularaemia: Bioterrorism defence renews interest in Francisella tularensis. *Nature Reviews Microbiology*. 2004;2:967-978.
9. Evans ME, Gregory DW, Schaffner W and McGee ZA. Tularemia - A 30-year Experience with 88 Cases. *Medicine*. 1985;64:251-269.
10. Cheng AC and Currie BJ. Melioidosis: Epidemiology, Pathophysiology, and Management. *Clinical Microbiology Reviews*. 2005;18:383-416.
11. Wiersinga WJ, Currie BJ and Peacock SJ. Melioidosis. *The New England journal of medicine*. 2012;367:1035-44.
12. Dance D. Treatment and prophylaxis of melioidosis. *Int J Antimicrob Agents*. 2014;43:310-8.
13. Wiersinga WJ, van der Poll T, White NJ, Day NP and Peacock SJ. Melioidosis: insights into the pathogenicity of Burkholderia pseudomallei. *Nature reviews Microbiology*. 2006;4:272-82.
14. Chaowagul W, Suputtamongkol Y, Dance DAB, Rajchanuvong A, Pattaraarechachai J and White NJ. Relapse in Melioidosis - Incidence and Risk-Factors. *Journal of Infectious Diseases*. 1993;168:1181-1185.
15. White NJ. Melioidosis. *Lancet*. 2003;361:1715-1722.
16. Clemens DL, Lee BY and Horwitz MA. Virulent and avirulent strains of Francisella tularensis prevent acidification and maturation of their phagosomes and escape into the cytoplasm in human macrophages. *Infection and Immunity*. 2004;72:3204-3217.
17. Sjostedt A. Intracellular survival mechanisms of Francisella tularensis, a stealth pathogen. *Microbes and Infection*. 2006;8:561-567.
18. Asare R and Abu Kwaik Y. Molecular complexity orchestrates modulation of phagosome biogenesis and escape to the cytosol of macrophages by Francisella tularensis. *Environmental Microbiology*. 2010;12:2559-2586.
19. Bosio CM, Bielefeldt-Ohmann H and Belisle JT. Active suppression of the pulmonary immune response by Francisella tularensis Schu4. *J Immunol*. 2007;178:4538-4547.
20. Matsuura M. Structural modifications of bacterial lipopolysaccharide that facilitate Gram-negative bacteria evasion of host innate immunity. *Front Immunol*. 2013;4:9.
21. Elkins KL, Leiby DA, Winegar RK, Nacy CA and Fortier AH. Rapid Generation of Specific Protective Immunity to Francisella-Tularensis. *Infection and Immunity*. 1992;60:4571-4577.
22. Steinmetz I, Rohde M and Brenneke B. Purification and Characterization of an Exopolysaccharide of Burkholderia (Pseudomonas) Pseudomallei. *Infection and Immunity*. 1995;63:3959-3965.

23. Stevens MP, Haque A, Atkins T, Hill J, Wood MW, Easton A, Nelson M, Underwood-Fowler C, Titball RW, Bancroft GJ and Galyov EE. Attenuated virulence and protective efficacy of a Burkholderia pseudomallei bsa type III secretion mutant in murine models of melioidosis. *Microbiology-Sgm*. 2004;150:2669-2676.

24. Harley VS, Dance DAB, Drasar BS and Tovey G. Effects of Burkholderia pseudomallei and other Burkholderia species on eukaryotic cells in tissue culture. *Microbios*. 1998;96:71-93.

25. Jones AL, Beveridge TJ and Woods DE. Intracellular survival of Burkholderia pseudomallei. *Infection and Immunity*. 1996;64:782-790.

26. Kespichayawattana W, Rattanachetkul S, Wanun T, Utaisincharoen P and Sirisinha S. Burkholderia pseudomallei induces cell fusion and actin-associated membrane protrusion: a possible mechanism for cell-to-cell spreading. *Infection and Immunity*. 2000;68:5377-5384.

27. Dennis DT, Inglesby TV, Henderson DA, Bartlett JG, Ascher MS, Eitzen E, Fine AD, Friedlander AM, Hauer J, Layton M, Lillibridge SR, McDade JE, Osterholm MT, O'Toole T, Parker G, Perl TM, Russell PK and Tonat K. Tularemia as a Biological Weapon: Medical and Public Health Management. *Journal of the American Medical Association*. 2001;285:2763-2773.

28. Gilad J, Harary I, Dushnitsky T, Schwartz D and Amsalem Y. Burkholderia mallei and Burkholderia pseudomallei as bioterrorism agents: National aspects of emergency preparedness. *Israel Medical Association Journal*. 2007;9:499-503.

29. CDC. Select Agents and Toxins List. 2014;2014.

30. Darling RG, Catlett CL, Huebner KD and Jarrett DG. Threats in bioterrorism I: CDC category A agents. *Emergency Medicine Clinics of North America*. 2002;20:273-+.

31. Greenfield RA and Bronze MS. Prevention and treatment of bacterial diseases caused by bacterial bioterrorism threat agents. *Drug Discov Today*. 2003;8:881-8.

32. Gilligan PH. The development of antimicrobials and vaccines against bacterial bioterrorism agents - Where are we? *Drug Discov Today*. 2004;9:205-206.

33. Ikaheimo I, Syrjala H, Karhukorpi J, Schildt R and Koskela M. In vitro antibiotic susceptibility of Francisella tularensis isolated from humans and animals. *Journal of Antimicrobial Chemotherapy*. 2000;46:287-290.

34. Tarnvik A and Chu MC. New Approaches to Diagnosis and Therapy of Tularemia. *Annals of the New York Academy of Science*. 2007;1105:378-404.

35. (WHO) WHO. Pneumonia Fact Sheet. 2016.

36. Vidyalakshmi K, Chakrapani M, Shrikala B, Damodar S, Lipika S and Vishal S. Tuberculosis mimicked by melioidosis. *Int J Tuberc Lung Dis*. 2008;12:1209-1215.

37. Thibault FM, Hernandez E, Vidal DR, Girardet M and Cavallo JD. Antibiotic susceptibility of 65 isolates of Burkholderia pseudomallei and Burkholderia mallei to 35 antimicrobial agents. *The Journal of antimicrobial chemotherapy*. 2004;54:1134-8.

38. Lau SKP, Sridhar S, Ho C-C, Chow W-N, Lee K-C, Lam C-W, Yuen K-Y and Woo PCY. Laboratory diagnosis of melioidosis: Past, present and future. *Experimental Biology and Medicine*. 2015;240:742-751.

39. Chaignat V, Djordjevic-Spasic M, Ruettger A, Otto P, Klimpel D, Muller W, Sachse K, Araj G, Diller R and Tomaso H. Performance of seven serological assays for diagnosing tularemia. *BMC Infect Dis*. 2014;14:6.

40. Kranz H and Bodmeier R. A novel in situ forming drug delivery system for controlled parenteral drug delivery. *International journal of pharmaceutics*. 2007;332:107-114.

41. Stebbins ND, Ouimet MA and Uhrich KE. Antibiotic-containing polymers for localized, sustained drug delivery. *Advanced Drug Delivery Reviews*. 2014;30:77-87.

42. Torchilin VP. Recent approaches to intracellular delivery of drugs and DNA and organelle targeting. *Annual review of biomedical engineering*. 2006;8:343-75.

43. O'Sullivan BP, Yasothan U and Kirkpatrick P. Inhaled aztreonam. *Nature Reviews Drug Discovery*. 2010;9:357-358.

44. Geller DE, Pitlick WH, Nardella PA, Tracewell WG and Ramsey BW. Pharmacokinetics and bioavailability of aerosolized tobramycin in cystic fibrosis. *Chest*. 2002;122:219-226.

45. Pai VB and Nahata MC. Efficacy and safety of aerosolized tobramycin in cystic fibrosis. *Pediatr Pulmonol*. 2001;32:314-327.

46. McCoy KS, Quittner AL, Oermann CM, Gibson RL, Retsch-Bogart GZ and Montgomery AB. Inhaled Aztreonam Lysine for Chronic Airway Pseudomonas aeruginosa in Cystic Fibrosis. *American Journal of Respiratory and Critical Care Medicine*. 2008;178:921-928.

47. Gibson RL, Retsch-Bogart GZ, Oermann C, Milla C, Pilewski J, Daines C, Ahrens R, Leon K, Cohen M, McNamara S, Callahan TL, Markus R and Burns JL. Microbiology, safety, and pharmacokinetics of aztreonam lysinate for inhalation in patients with cystic fibrosis. *Pediatr Pulmonol*. 2006;41:656-665.

48. Labiris NR and Dolovich MB. Pulmonary drug delivery. Part I: Physiological factors affecting therapeutic effectiveness of aerosolized medications. *British Journal of Clinical Pharmacology*. 2003;56:588-599.

49. Mansour HM, Rhee YS and Wu XA. Nanomedicine in pulmonary delivery. *International Journal of Nanomedicine*. 2009;4:299-319.

50. Chocarro A, Gonzalez A and Carcia I. Treatment of tularemia with Ciprofloxacin. *Clinical Infectious Diseases*. 2000;31:623-623.

51. Torchilin VP. Micellar nanocarriers: Pharmaceutical perspectives. *Pharmaceutical research*. 2007;24:1-16.

52. Hamblina KA, Armstronga SJ, Barnesa KB, Daviesa C, Wong JP, Blanchard JD, Hardinga SV, Simpson AJH and Atkins HS. Liposome Encapsulation of Ciprofloxacin Improves Protection against Highly Virulent Francisella tularensis Strain Schu S4. *Antimicrobial Agents and Chemotherapy*. 2014;58:3053-3059.

53. Cipolla D, Blanchard J and Gonda I. Development of Liposomal Ciprofloxacin to Treat Lung Infections. *Pharmaceutics*. 2016;8.

54. Pilcer G and Amighi K. Formulation strategy and use of excipients in pulmonary drug delivery. *International journal of pharmaceutics*. 2010;392:1-19.

55. Torchilin VP. Recent advances with liposomes as pharmaceutical carriers. *Nature Reviews Drug Discovery*. 2005;4:145-160.

56. Sharma A and Sharma US. Liposomes in drug delivery: progress and limitations. *International journal of pharmaceutics*. 1997;154:123-140.

57. Uhrich KE, Cannizzaro SM, Langer RS and Shakesheff KM. Polymeric Systems for Controlled Drug Release. *Chemical Reviews*. 1999;99:3181-3198.

58. Kataoka K, Harada A and Nagasaki Y. Block copolymer micelles for drug delivery: design, characterization and biological significance. *Advanced Drug Delivery Reviews*. 2001;47:113-131.

59. Ungaro F, d' Angelo I, Miro A, La Rotonda MI and Quaglia F. Engineered PLGA nano- and micro-carriers for pulmonary delivery: challenges and promises. *Journal of Pharmacy and Pharmacology*. 2012;64:1217-1235.

60. Arnold MM, Gonnan EM, Schieber LJ, Munson EJ and Berkland C. NanoCipro encapsulation in monodisperse large porous PLGA microparticles. *Journal of Controlled Release*. 2007;121:100-109.

61. Chow AH, Tong HH, Chattopadhyay P and Shekunov BY. Particle engineering for pulmonary drug delivery. *Pharmaceutical research*. 2007;24:411-37.

62. Sobczak M. Synthesis and characterization of polyester conjugates of ciprofloxacin. *European Journal of Medicinal Chemistry*. 2010;45:3844-3849.

63. Amly W and Karaman R. Recent updates in utilizing prodrugs in drug delivery (2013-2015). *Expert opinion on drug delivery*. 2016;13:571-91.

64. Stella VJ, Charman WNA and Naringrekar VH. Prodrugs - Do They Have Advantages in Clinical Practice? *Drugs*. 1985;29:455-473.

65. Shen YQ, Jin EL, Zhang B, Murphy CJ, Sui MH, Zhao J, Wang JQ, Tang JB, Fan MH, Van Kirk E and Murdoch WJ. Prodrugs Forming High Drug Loading Multifunctional Nanocapsules for Intracellular Cancer Drug Delivery. *J Am Chem Soc*. 2010;132:4259-4265.

66. Alexander J, Fromtling RA, Bland JA, Pelak BA and Gilfillan EC. (Acyloxy)Alkyl Carbamate Prodrugs of Norfloxacin. *J Med Chem*. 1991;34:78-81.

67. Coessens V, Schacht EH and Domurado D. Synthesis and in vitro stability of macromolecular prodrugs of norfloxacin. *Journal of Controlled Release*. 1997;47:283-291.

68. Chiefari J, Chong YK, Ercole F, Krstina J, Jeffery J, Le TPT, Mayadunne RTA, Meijs GF, Moad CL, Moad G, Rizzardo E and Thang SH. Living free-radical polymerization by reversible addition-fragmentation chain transfer: The RAFT process. *Macromolecules*. 1998;31:5559-5562.

69. Gregory A and Stenzel M. Complex polymer architectures via RAFT polymerization: From fundamental process to extending the scope using click chemistry and nature's building blocks. *Progress in polymer science*. 2012;37:38-105.

70. Kryger MBL, Wohl BM, Smith AAA and Zelikin AN. Macromolecular prodrugs of ribavirin combat side effects and toxicity with no loss of activity of the drug. *Chemical Communications*. 2013;49:2643-2645.

71. Das D, Srinivasan S, Kelly AM, Chiu DY, Daugherty BK, Ratner DM, Stayton PS and Convertine AJ. RAFT polymerization of ciprofloxacin prodrug monomers for the controlled inracellular delivery of antibiotics. *Polymer Chemistry*. 2016;Advance Article.

72. Das D, Chen J, Srinivasan S, Kelly AM, Lee B, Son H-N, Radella F, West TE, Ratner DM, Convertine AJ, Skerrett SJ and Stayton PS. Synthetic Macromolecular Antibiotic Platform for Inhalable Therapy against Aerosolized Intracellular Alveolar Infections. *Molecular Pharmaceutics*. 2017;14:1988-1997.

73. Chen J. Glycan polymeric prodrugs against pulmonary intracellular alveolar infections. *Bioengineering*. 2017;PhD.

74. Yang W, Liu SJ, Bai T, Keefe AJ, Zhang L, Ella-Menye JR, Li YT and Jiang SY. Poly(carboxybetaine) nanomaterials enable long circulation and prevent polymer-specific antibody production. *Nano Today*. 2014;9:10-16.

75. Zylberberg C and Matosevic S. Pharmaceutical liposomal drug delivery: a review of new delivery systems and a look at the regulatory landscape. *Drug Deliv*. 2016;23:3319-3329.

76. Geller DE, Weers J and Heuerding S. Development of an Inhaled Dry-Powder Formulation of Tobramycin Using PulmoSphere™ Technology. *Journal of Aerosol Medicine and Pulmonary Drug Delivery*. 2011;24:175-182.

77. Newman SP. Dry powder inhalers for optimal drug delivery. *Expert opinion on biological therapy*. 2004;4:23-33.

78. Hallaj-Nezhadi S and Hassan M. Nanoliposome-based antibacterial drug delivery. *Drug Deliv*. 2015;22:581-589.

79. Sercombe L, Veerati T, Moheimani F, Wu SY, Sood AK and Hua S. Advances and Challenges of Liposome Assisted Drug Delivery. *Frontiers in Pharmacology*. 2015;6:286.

80. Drulis-Kawa Z and Dorotkiewicz-Jach A. Liposomes as delivery systems for antibiotics. *International journal of pharmaceutics*. 2010;387:187-198.

81. Gregoriadis G. Engineering liposomes for drug delivery: progress and problems. *Trends in Biotechnology*. 1995;13:527-537.

82. Noel S, Gasser V, Pesset B, Hoegy F, Rognan D, Schalk IJ and Mislin GLA. Synthesis and biological properties of conjugates between fluoroquinolones and a N3 "-functionalized pyochelin. *Org Biomol Chem*. 2011;9:8288-8300.

83. Reeves BD, Young M, Grieco PA and Suci P. Aggregatibacter actinomycetemcomitans biofilm killing by a targeted ciprofloxacin prodrug. *Biofouling*. 2013;29:10.1080/08927014.2013.823541.

84. Chen J, Son HN, Hill JJ, Srinivasan S, Su FY, Stayton PS, Convertine AJ and Ratner DM. Nanostructured glycopolymer augmented liposomes to elucidate carbohydrate-mediated targeting. *Nanomedicine : nanotechnology, biology, and medicine*. 2016;12:2031-2041.

85. Chakraborty P, Bhaduri AN and Das PK. Sugar receptor mediated drug delivery to macrophages in the therapy of experimental visceral leishmaniasis. *Biochemical and Biophysical Research Communications*. 1990;166:404-410.

86. De Carvalho PB, Ramos DC, Cotrim PC and Ferreira EI. Synthesis and in vitro evaluation of potential anti-leishmanial targeted drugs of pyrimethamine. *Journal of pharmaceutical sciences*. 2003;92:2109-16.

87. Kapoor G, Saigal S and Elongavan A. Action and resistance mechanisms of antibiotics: A guide for clinicians. *Journal of anaesthesiology, clinical pharmacology*. 2017;33:300-305.

88. Pinder N, Brenner T, Swoboda S, Weigand MA and Hoppe-Tichy T. Therapeutic drug monitoring of beta-lactam antibiotics - Influence of sample stability on the analysis of piperacillin, meropenem, ceftazidime and flucloxacillin by HPLC-UV. *Journal of pharmaceutical and biomedical analysis*. 2017;143:86-93.

89. Fidock DA, Rosenthal PJ, Croft SL, Brun R and Nwaka S. Antimalarial drug discovery: efficacy models for compound screening. *Nature Reviews Drug Discovery*. 2004;3:509.

90. Tallarida RJ. An Overview of Drug Combination Analysis with Isobolograms. *Journal of Pharmacology and Experimental Therapeutics*. 2006;319:1.

91. Weinstein Z and H. Zaman M. *Quantitative bioassay to identify antimicrobial drugs through drug interaction fingerprint analysis*; 2017.

92. Ulrich RL, Deshazer D, Kenny TA, Ulrich MP, Moravusova A, Opperman T, Bavari S, Bowlin TL, Moir DT and Panchal RG. Characterization of the Burkholderia thailandensis SOS response by using whole-transcriptome shotgun sequencing. *Applied and environmental microbiology*. 2013;79:5830-43.

93. Inglis TJ, Rodrigues F, Rigby P, Norton R and Currie BJ. Comparison of the susceptibilities of Burkholderia pseudomallei to meropenem and ceftazidime by conventional and intracellular methods. *Antimicrob Agents Chemother*. 2004;48:2999-3005.

94. Labro MT. Interference of antibacterial agents with phagocyte functions: immunomodulation or "immuno-fairy tales"? *Clin Microbiol Rev*. 2000;13:615-50.

95. Chou TC. Drug combination studies and their synergy quantification using the Chou-Talalay method. *Cancer research*. 2010;70:440-6.

96. Nazli E, Zer Y and Eksi F. In vitro efficacy of various antibiotic combinations against Pseudomonas aeruginosa isolates. *The Journal of international medical research*. 2015;43:217-25.

97. Zhou J, Chen Y, Tabibi S, Alba L, Garber E and Saiman L. Antimicrobial susceptibility and synergy studies of Burkholderia cepacia complex isolated from patients with cystic fibrosis. *Antimicrob Agents Chemother*. 2007;51:1085-8.

98. Liu W, Wan J, Han JZ, Li C, Feng DD, Yue SJ, Huang YH, Chen Y, Cheng QM, Li Y and Luo ZQ. Antiflammin-1 attenuates bleomycin-induced pulmonary fibrosis in mice. *Respir Res*. 2013;14:101.

99. Das D, Gerboth D, Postma A, Srinivasan S, Kern H, Chen J, Ratner DM, Stayton PS and Convertine AJ. Synthesis of zwitterionic, hydrophobic, and amphiphilic polymers via RAFT polymerization induced self-assembly (PISA) in acetic acid. *Polymer Chemistry*. 2016;7:6133-6143.

100. Imani S, Buscher H, Marriott D, Gentili S and Sandaradura I. Too much of a good thing: a retrospective study of β-lactam concentration–toxicity relationships. *Journal of Antimicrobial Chemotherapy*. 2017;72:2891-2897.

101. Hatem NA, Campbell S, Rubio E and Loschner AL. Meropenem: A possible new culprit in eosinophilic lung diseases. *Lung India*. 2017;34:461-464.

102. Bleyer M, Curths C, Dahlmann F, Wichmann J, Bauer N, Moritz A, Braun A, Knauf S, Kaup FJ and Gruber-Dujardin E. Morphology and staining behavior of neutrophilic and eosinophilic granulocytes of the common marmoset (Callithrix jacchus). *Experimental and toxicologic pathology : official journal of the Gesellschaft fur Toxikologische Pathologie*. 2016;68:335-43.